Neurobiology of Disease 206 (2025) 106817

Contents lists available at ScienceDirect

Neurobiology of Disease

journal homepage: www.elsevier.com/locate/ynbdi

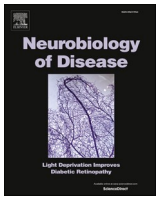

S100A9 protein activates microglia and stimulates phagocytosis, resulting in synaptic and neuronal loss

Katryna Pampuscenko [a,*], Silvija Jankeviciute [a], Ramune Morkuniene [a], Darius Sulskis [b], Vytautas Smirnovas [b], Guy C. Brown [c], Vilmante Borutaite [a]

[a] Neuroscience Institute, Lithuanian University of Health Sciences, LT-50161 Kaunas, Lithuania
[b] Life Sciences Center, Institute of Biotechnology, Vilnius University, LT-10257 Vilnius, Lithuania
[c] Department of Biochemistry, University of Cambridge, Cambridge CB2 1QW, United Kingdom

ARTICLE INFO

Keywords:
S100A9 protein
Cell death
Neurotoxicity
Neuroinflammation
Microglia
Neurodegeneration

ABSTRACT

S100 calcium-binding protein A9 (S100A9, also known as calgranulin B) is expressed and secreted by myeloid cells under inflammatory conditions, and S100A9 can amplify inflammation. There is a large increase in S100A9 expression in the brains of patients with neurodegenerative diseases, such as Alzheimer's disease, and S100A9 has been suggested to contribute to neurodegeneration, but the mechanisms are unclear. Here we investigated the effects of extracellular recombinant S100A9 protein on microglia, neurons and synapses in primary rat brain neuronal-glial cell cultures. Incubation of cell cultures with 250–500 nM S100A9 caused neuronal loss without signs of apoptosis or necrosis, but accompanied by exposure of the "eat-me" signal - phosphatidylserine on neurons. S100A9 caused activation of microglial inflammation as evidenced by an increase in the microglial number, morphological changes, release of pro-inflammatory cytokines, and increased phagocytic activity. At lower concentrations, 10–100 nM S100A9 induced synaptic loss in the cultures. Depletion of microglia from the cultures prevented S100A9-induced neuronal and synaptic loss, indicating that neuronal and synaptic loss was mediated by microglia. These results suggest that extracellular S100A9 may contribute to neurodegeneration by activating microglial inflammation and phagocytosis, resulting in loss of synapses and neurons. This further suggests the possibility that neurodegeneration may be reduced by targeting S100A9 or microglia.

1. Introduction

Neurodegenerative disorders, such as Alzheimer's disease (AD), Parkinson's disease (PD), Huntington's diseases and amyotrophic lateral sclerosis, are mainly characterized by progressive protein misfolding, neuroinflammation, synapse loss, neuronal loss and clinical symptoms, usually in that order (Dong-Chen et al., 2023; Guo et al., 2020). Although misfolding of specific proteins is considered as the primary initiator of neurodegeneration (Wilson et al., 2023), clinical trials based on removing such proteins have had limited success so far (Asher and Priefer, 2022; Xiao and Tan, 2023). This suggests that targeting neuroinflammation, synapse loss and neuronal loss, may be beneficial, particularly for patients who already have clinical symptoms (Kwon et al., 2020). Currently, neuroinflammation is attracting significant

Abbreviations: AD, Alzheimer's disease; Ara-C, cytosine β- D–arabinofuranoside; Aβ, beta-amyloid; BSA, bovine serum albumin; bzATP, (2′(3′)-O-(4-Benzoyl-benzoyl)adenosine-5′-triphosphate; CNS, central nervous system; DIV, days in vitro; DMEM, Dulbecco's modified Eagle's medium; ELISA, enzyme-linked immunosorbent assay; FBS, fetal bovine serum; GFAP, glial fibrillary acidic protein; HEPES, 4-(2-hydroxyethyl)-1-piperazineethanesulfonic acid; Iba-1, ionized calcium-binding adaptor molecule 1; IgG, immunoglobulin G; IL-1β, interleukin-1 beta; LAL, *Limulus* Amebocyte Lysate; LDS, lithium dodecyl-sulfate; LME, L-Leucine methyl ester; LPS, lipopolysaccharide; MAP2, microtubule-associated protein 2; MRP14, myeloid-related protein 14; NF-κB, nuclear factor kappa-light-chain-enhancer of activated B cells; NO, nitric oxide; PBS, phosphate buffered saline; PD, Parkinson's disease; PSD-95, postsynaptic density protein 95; PVDF, polyvinylidene fluoride; RAGE, receptor for advanced glycation end products; SDS, sodium dodecyl-sulfate; SD, standard deviation; Tau, tubulin-associated unit; TLR4, Toll-like receptor 4; TNF-α, tumor necrosis factor alpha.

* Corresponding author.
E-mail addresses: katryna.pampuscenko@lsmu.lt (K. Pampuscenko), silvija.jankeviciute@lsmu.lt (S. Jankeviciute), ramune.morkuniene@lsmu.lt (R. Morkuniene), darius.sulskis@gmc.vu.lt (D. Sulskis), vytautas.smirnovas@bti.vu.lt (V. Smirnovas), gcb3@cam.ac.uk (G.C. Brown), vilmante.borutaite@lsmu.lt (V. Borutaite).

https://doi.org/10.1016/j.nbd.2025.106817
Received 22 August 2024; Received in revised form 24 January 2025; Accepted 27 January 2025
Available online 28 January 2025

interest as a potential therapeutic target for neurodegenerative diseases (Bartels et al., 2020; Liu et al., 2022; Zhang et al., 2023a, 2023b). Neuroinflammation can be initiated by pathological protein aggregates, however, inflammatory reactions can promote protein misfolding and can arise prior to neurodegeneration (Zhang et al., 2023a, 2023b). Therefore, a more detailed understanding of the molecular mechanisms and factors leading to neuroinflammation and subsequent neurodegeneration may be beneficial.

There is growing evidence that the pro-inflammatory S100A9 protein is upregulated during neurodegeneration and may contribute to neurodegenerative processes (Andrade-Talavera et al., 2022; Gruden et al., 2016; Horvath et al., 2018; Wang et al., 2018a, 2018b; Zhang et al., 2023a). S100A9, also known as calgranulin B or myeloid-related protein 14 (MRP14), is a protein that belongs to the S100 protein family and is primarily expressed in myeloid cells in response to pro-inflammatory triggers (Wang et al., 2018a, 2018b). Released S100A9 plays an important role in immune responses by recruiting and activating nearby immune cells through binding to Toll-like receptor 4 (TLR4) and Receptor for Advanced Glycation End Products (RAGE), and thereby inducing cytokine production (Garcia et al., 2022). As a result, S100A9 can create a positive feedback loop, where inflammation induces S100A9 secretion, which in turn promotes further inflammation (Garcia et al., 2022; Wang et al., 2018a, 2018b). The chronic inflammation associated with aging may in part cause or be caused by the robust elevation of S100A9 expression in different cell types including the central nervous system (CNS) during aging (Swindell et al., 2013). Notably, S100A9 has been found to be highly upregulated in the brains of AD and PD patients (Chang et al., 2012; Horvath et al., 2018; Kummer et al., 2012), with more than a 9-fold increase in S100A9 levels in whole-brain lysates of AD patients compared to the age-matched control group (Kummer et al., 2012). In transgenic mouse models, pathological AD-related protein changes were suggested to arise from S100A9-mediated neuroinflammation (Kummer et al., 2012; Wang et al., 2018a, 2018b). Neuroinflammation is regulated by microglia, a type of CNS macrophage, and S100A9 was found to induce microglial inflammation in the BV-2 microglial cell line through TLR4/NF-κB signalling (Zhang et al., 2023a, 2023b). Thus, in the context of neurodegeneration, S100A9 may serve as a critical factor mediating neuroinflammation. S100A9 is a relatively unstable protein, which can form amyloidogenic oligomers and fibrils, and there is evidence that these can be neurotoxic (Wang et al., 2014), but the mechanism of this neurotoxicity is unclear.

Neuronal damage and death in neurodegenerative diseases may proceed via various mechanisms, including neuronal damage and death caused by microglial activation and neuroinflammation (Bartels et al., 2020; Fricker et al., 2018; Gao et al., 2023). When activated by pathological factors, microglia become highly phagocytic, and excessive microglial phagocytosis can lead to the elimination of functional synapses and neurons. Microglial phagocytosis of an otherwise-viable neuron results in death of the engulfed neuron within the microglia – a form of cell death that is known as ‘cell death by phagocytosis’ or ‘phagoptosis’ for short. Phagoptosis is one of the most common forms of cell death in mammals, and occurs when stressed, activated, damaged, aged or excess cells expose “eat-me” signals that induce phagocytes to phagocytose such cells (Brown, 2024; Butler et al., 2021). Phagoptosis is increased by inflammation because inflammation increases oxidative stress, phagocytosis, phagocytic receptors and the release of opsonins by phagocytes (Brown, 2024). Neuronal death by phagocytic uptake can occur in a variety of contexts, such as tau pathology (Brelstaff et al., 2018; Pampuscenko et al., 2020, 2021, 2023; Puigdellívol et al., 2021) amyloid beta (Aβ) pathology (Neniskyte et al., 2011, 2016; Neniskyte and Brown, 2013a), prion disease (Sinha et al., 2021), Gaucher disease (Shimizu et al., 2023), retinal degeneration (Zhao et al., 2015), bacterial lipoteichoic acid- or lipopolysaccharide (LPS)-induced inflammation (Kinsner et al., 2006; Milde et al., 2021; Neher et al., 2011), epilepsy (Umpierre et al., 2024) and brain ischemia (Brown, 2021; Milde and Brown, 2022; Neher et al., 2013). S100A9 has been reported to increase phagocytosis by BV-2 microglia at low concentrations, and inhibit phagocytosis at higher concentrations of S100A9 (Zhang et al., 2023a, 2023b), however it is not clear whether and how S100A9-induced activation of microglia contributes to neurodegeneration. Therefore, it may be useful to further investigate the role of S100A9 in inflammation-mediated neurodegeneration and its potential as a target for therapeutic interventions.

In this study, we focus on the potential role of S100A9 in microglial activation and neurotoxicity, which may contribute to neurodegeneration. For the first time, we show that extracellular, oligomerized S100A9 induces neuronal and synaptic loss due to microglial phagocytosis.

2. Materials and methods

2.1. Materials and reagents

E. coli BL21 Star (DE3) cells (Cat# C601003), DMEM Glutamax (Cat# 61965–026), horse serum (Cat# 16050122), fetal bovine serum (Cat# A3840401), penicillin – streptomycin (Cat# 15140122), Versene (1:5000) solution (Cat# 15040066), anti-S100A9 (Cat# PA1–46489), anti-NeuN (Cat# MA5–33103), anti-Iba-1 (Cat# PA5–18039), anti-GFAP (Cat# MA5–12023), anti-PSD95 (Cat# MA5–41092), anti-synapsin 1 (Cat# MA5–31919), anti-CD68 (Cat# MA5–13324), anti-Rabbit IgG (H + L) Highly Cross-Adsorbed Secondary Antibody Alexa Fluor™ Plus 555 (Cat# A32732), Goat anti-Mouse IgG (H + L) Superclonal™ Recombinant Secondary Antibody Alexa Fluor™ 488 (Cat# A28175), isolectin GS-IB_4-AlexaFluor488 conjugate (Cat# I21411), TNF-α ELISA kit (Cat# BMS622), Griess reagent kit (Cat# G7921), NuPAGE LDS sample buffer (#NP0007), Novex Sharp Pre-stained Protein Standard (Cat# LC5800), Pierce Chromogenic Endotoxin Quant Kit (Cat# A39552) were purchased from Invitrogen, ThermoFisher Scientific or Thermo Scientific. L-Leucine methyl ester (Cat# L1002), Hoechst33342 (Cat# B2261), propidium iodide (Cat# P4170), carboxylate-modified 2 μm latex beads (Cat# L3030), phenylmethylsulfonyl fluoride (Cat# 11359061001), lysozyme (Cat# L6876) were from Sigma-Aldrich. IL-1β ELISA kit (Cat# abx050112) was from Abbexa, Annexin V-Cy3 conjugate (Cat#14143) from Abcam, poly-(L)-lysine (Cat# 3438–200-01) from Cultrex, R&D systems (USA), bzATP (2′(3′)-O-(4-Benzoylbenzoyl)adenosine-5′-triphosphate, tri(triethylammonium) salt (Cat# HY-136254) was from MedChemExpress, DEAE Sepharose (Cat# 17070901), HiLoad 26/600 Superdex 75 prep grade column (Cat# 28989334) were from Cytiva and 10 kDa molecular weight cutoff (Cat# UFC901008) was from Merck Millipore.

2.2. Expression and purification of recombinant S100A9 protein

S100A9 was expressed and purified as previously described (Hunter and Chazin, 1998) with slight modifications. In brief, the protein was expressed in *E. coli* BL21 Star (DE3) cells (Thermo Scientific) as inclusion bodies. The cells were cultured in 2 L of ZYM-5052 auto-induction medium (Studier, 2005) supplemented with 100 μg/mL ampicillin at 37 °C for 4 h, followed by overnight incubation at 25 °C. Cells were harvested by centrifugation at 6000*g* for 25 min at 4 °C and resuspended in PBS buffer containing 1 mM phenylmethylsulfonyl fluoride (Sigma-Aldrich) and 0.2 mg/mL lysozyme (Sigma-Aldrich). The suspension was lysed via sonication (15 s on, 30 s off, 40 % amplitude) and the lysate was centrifuged at 18,000*g* for 45 min at 4 °C.

The resulting pellet was washed with 1 M urea and centrifuged again at 18,000*g* for 45 min at 4 °C. Inclusion bodies were solubilized in 6 M guanidine hydrochloride, and the protein was refolded by dialysis three times against a refolding buffer (20 mM Tris-HCl, 1 mM EDTA, 0.5 mM DTT, pH 8) at 8 °C overnight. After refolding, insoluble debris was removed by centrifugation at 18,000*g* for 45 min at 4 °C.

The supernatant was applied onto a DEAE Sepharose (Cytiva) loaded column pre-equilibrated with wash buffer (20 mM Tris-HCl, 0.5 mM

DTT, pH 8). S100A9 was eluted using a step-wise gradient with elution buffer (20 mM Tris-HCl, 0.5 M NaCl, 0.5 mM DTT, pH 8). Fractions containing the protein were concentrated using Amicon centrifugal filters with a 10 kDa molecular weight cutoff (MWCO; Merck Millipore).

Prior to size exclusion chromatography, the protein sample was incubated with 5 mM DTT and 5 mM EDTA for 30 min on ice. The sample was then loaded onto a HiLoad 26/600 Superdex 75 prep grade column (Cytiva) pre-calibrated with gel-filtration buffer (25 mM ammonium bicarbonate, pH 7.2). The fractions containing S100A9 were collected, lyophilized, and stored at −80 °C. Endotoxin level in recombinant S100A9 protein samples was evaluated using *Limulus* amebocyte lysate (LAL) assay and manufacturer's (Pierce Chromogenic Endotoxin Quant Kit, ThermoScientific) provided protocol. The endotoxin levels were equal to or less than 0.004 % (*w/v*).

2.3. S100A9 preparation for cell culture treatments

Lyophilized recombinant S100A9 was dissolved in PBS at 0.138 mg/mL concentration. This dilution was referred to as protocol I. Protein solutions were aliquoted and stored at −80 °C. To induce protein oligomerization, recombinant S100A9 was pre-incubated at room temperature for 30 min (protocol II), 6 h (protocol III) and 24 h (protocol IV) with continuous agitation on an orbital shaker at 25 rpm speed. Cell cultures were treated with 10 nM – 2 μM S100A9 protein. The molecular concentration of S100A9 was calculated according to the theoretical molecular weight of monomeric protein form (Mr = 13,200 Da).

2.4. S100A9 protein characterization by non-reducing SDS-PAGE and Western blot analysis

The aggregation state of recombinant human S100A9 protein was determined by non-reducing SDS-PAGE and Western blot analysis. For electrophoresis, S100A9 protein samples (300 ng) were supplemented with NuPAGE LDS (Invitrogen, ThermoFisher Scientific) sample buffer without heating and reductive agents. Samples were separated using 10 % Tris-Glycine gel and 25 mM Tris base, 192 mM Glycine, 0.1 % SDS running buffer. Resolved proteins were then transferred onto polyvinylidene fluoride (PVDF; 0.45 μm) membrane using 24 mM Tris base, 192 mM Glycine transfer buffer. Membrane was probed with primary anti-S100A9 antibody (1:1000) overnight (4 °C) after blocking with 5 % bovine serum albumin (BSA) solution. Chemiluminescent detection was carried out using ready-to-use alkaline phosphatase-conjugated anti-rabbit secondary antibody (Invitrogen) and chemiluminescent CDP-Star substrate (Invitrogen). Membrane imaging was performed using UVP imaging system and Vision WorksLS Software. Protein band densitometry was carried out using ImageJ 1.8.0 software (Schneider et al., 2012).

2.5. Primary rat brain cell cultures

Experimental procedures involving animals were undertaken in accordance with the EU Directive 2010/63/EU for animal experiments and the Republic of Lithuania law on the care, keeping, and use of experimental animals. Animal care and experimental procedures were approved by Lithuanian State Food and Veterinary Service (ethical approval No. G2–267).

Primary neuronal-glial co-cultures were prepared from postnatal 5–7 day Wistar rat pup cerebellum as described in (Bal-Price and Brown, 2001). Brain cerebellum were dissociated in Versene (1:5000) solution and plated at a density of 1,000,000 cells/mL in 48 well plates pre-coated with 1 μg/mL of poly-L-lysine. Cell cultures were plated and maintained in DMEM Glutamax culture medium supplemented with 5 % horse serum, 5 % fetal bovine serum (FBS), 10 units/mL penicillin-10 μg/mL streptomycin, 13 mM glucose and 20 mM KCl at 37 °C and 5 % CO_2 for 7–9 days prior experiments. Neuronal-glial co-cultures consisted of neurons 82 ± 3 % ($NeuN^+$), 5 ± 2 % microglia ($Iba\text{-}1^+$/isolectin-IB_4^+) and 13 ± 3 % astrocytes ($GFAP^+$) (Supplementary Fig. 1S A).

To eliminate microglia, neuronal-glial co-cultures were treated with 20 mM L-Leucine methyl ester (LME) at 6 days in vitro (DIV) (Jebelli et al., 2015). Following 4 h incubation the medium from each well was completely removed and replaced with medium from untreated cell cultures. Microglial-depleted cell cultures consisted of neurons 82 ± 1 % ($NeuN^+$), <1 % microglia (isolectin-$IB4^+$) and 18 ± 2 % astrocytes ($GFAP^+$) (Supplementary Fig. 1S B).

To eliminate glial cells, neuronal-glial co-cultures were treated with 10 μM of cytosine β- D–arabinofuranoside (Ara—C) at 2 DIV. Pure neuronal cultures consisted of 96 ± 1 % neurons.

Primary microglia cell mono-cultures were prepared from postnatal 5–7 day Wistar rat pup brain cortices as described previously (Pampuscenko et al., 2020). Brain cortices were dissociated in Versene (1:5000) and seeded into 75 T flasks coated with 0.5 μg/mL poly-(L)-lysine in DMEM-Glutamax supplemented with 10 % FBS and 10 units/mL penicillin-10 μg/mL streptomycin. After reaching confluence (approximately 7–10 days after seeding), microglial cell cultures were mechanically detached and plated at a density of 100,000 cells/mL into 48-well plates coated with 0.5 μg/mL poly-(L)-lysine. The microglial cells were allowed to attach overnight before any treatment. These cell cultures consisted of 96 ± 2 % microglia.

2.6. Neuronal viability assessment

Neuronal viability in co-cultures was assessed by double staining of nuclei (Supplementary Fig. 2S). Cell cultures were incubated with 4 μg/mL Hoechst 33342 and 7 ng/mL propidium iodide for 15 min (5 % CO_2, 37 °C). Neurons were distinguished in phase contrast images according to their specific shape and morphology. Cells stained homogeneously with Hoechst 33342 (blue) were considered viable, while those stained with propidium iodide (red) as necrotic. Cells with condensed or fragmented nuclei (Hoechst 33342, bright blue) were classified as undergoing apoptosis. Cell cultures were analysed with microscope (Olympus IX71S1F-3, USA) in 4–5 randomly chosen microscopic fields at 20 × magnification. Quantification was carried out using ImageJ 1.8.0 software (Schneider et al., 2012).

2.7. Microglia cell number and area assessment

Microglial cells in neuronal-glial co-cultures were labelled with 7 ng/mL isolectin GS-IB_4-AlexaFluor488 conjugate for 15 min (5 % CO_2, 37 °C). Cell cultures were analysed with microscope (Olympus IX71S1F-3, USA) in 4–5 randomly chosen microscopic fields at 10 × and 20 × magnifications. For microglial cell number assessment, total microglial cell number was calculated in fluorescence images at 10 × magnification. Microglial cell area was calculated in binary images at 20 × magnification and normalised to number of cells per field. Quantification was carried out using ImageJ 1.8.0 software (Schneider et al., 2012).

2.8. Phosphatidylserine staining with Annexin V-Cy3.18 conjugate

Neuronal-glial co-cultures were washed two times with PBS and then one time with Annexin V binding buffer containing 10 mM HEPES, 140 mM NaCl, and 2.5 mM $CaCl_2$ (pH of 7.5). Cell cultures were incubated with 4.5 μg/mL of Annexin V-Cy3 conjugate in binding buffer for 10 min at room temperature. To visualize cell nuclei and microglia, Hoechst 33342 (4 μg/mL) and isolectin GS-IB_4-AlexaFluor488 conjugate (7 ng/mL) were added. After incubation, cell cultures were washed with Annexin V binding buffer and fixed with 4 % paraformaldehyde for 15 min. Neuronal-glial co-cultures were analysed under a fluorescence microscope (Olympus IX71S1F-3, USA) in 4–5 randomly chosen microscopic fields at 20 × magnification. Annexin V-Cy3 fluorescence intensity was measured using ImageJ 1.8.0 software (Schneider et al., 2012) and normalised to 100 % for untreated neurons.

2.9. Evaluation of microglial phagocytic activity by latex beads

To determine microglial phagocytic activity microglial cell monocultures were incubated with 0.005 % (*w/v*) carboxylate-modified 2 μm latex beads for 2 h (5 % CO_2 and 37 °C). Afterwards, cell nuclei were stained with Hoechst 33342 (4 μg/mL) for 5 min. Cell cultures were washed with PBS buffer several times and then fixed with 4 % paraformaldehyde. The microglial cells were analysed under a fluorescence microscope (Olympus IX71S1F-3, USA) in 5–7 randomly chosen microscopic fields at 20 × magnification. The number of latex beads per microglial cell was calculated using ImageJ 1.8.0 software (Schneider et al., 2012).

2.10. Evaluation of Iba-1 expression, CD68 expression and synaptic density by immunofluorescence assay

Cell cultures were fixed with 4 % paraformaldehyde for 15 min following further blockage with 0.1 M glycine solution for 10 min. Cells were permeabilized with 0.1 % saponin for 10 min. All steps were performed at room temperature, and each step was followed by three washes with PBS. Non-specific interactions were blocked with 15 % BSA for 30 min at room temperature. Each well was rinsed with PBS and then cell cultures were incubated with primary antibodies overnight at 4 °C in PBS with 5 % BSA. After three PBS washes, the cells were incubated with the secondary antibodies in PBS with 5 % BSA for 2 h at room temperature.

For microglial labelling and evaluation of Iba-1 expression, primary anti-Iba-1 goat polyclonal antibody (Invitrogen, ThermoFisher Scientific) and Rabbit anti-Goat IgG (H + L) Cross-Adsorbed Secondary Antibody, Alexa Fluor™ 555 (Invitrogen, ThermoFisher Scientific) were used. Cell cultures were analysed under a fluorescence microscope (Olympus IX71S1F-3, USA) in 4–5 randomly chosen microscopic fields at 20 × magnification. The fluorescence intensity was measured using ImageJ 1.8.0 software (Schneider et al., 2012) and normalised to number of microglial cells per microscopic field.

For evaluation of CD68 expression, primary anti-CD68 monoclonal antibody KP1 (Invitrogen, ThermoFisher Scientific) and Goat anti-Mouse IgG (H + L), Superclonal™ Recombinant Secondary Antibody, Alexa Fluor™ 488 (Invitrogen, ThermoFisher Scientific) were used. Cell cultures were analysed under a fluorescence microscope (Olympus IX71S1F-3, USA) in 4–5 randomly chosen microscopic fields at 20 × magnification. The fluorescence intensity per cell was measured using ImageJ 1.8.0 software (Schneider et al., 2012).

For evaluation of synaptic puncta, primary antibodies anti-PSD95 rabbit monoclonal antibody (SR38–09) (Invitrogen, ThermoFisher Scientific) and anti-synapsin 1 mouse monoclonal antibody (7H10G6) (Invitrogen, ThermoFisher Scientific) were used for the immunofluorescence analysis. Secondary antibodies goat anti-Rabbit IgG (H + L) Highly Cross-Adsorbed Secondary Antibody, Alexa Fluor™ Plus 555 (Invitrogen, ThermoFisher Scientific) and Goat anti-Mouse IgG (H + L), Superclonal™ Recombinant Secondary Antibody, Alexa Fluor™ 488 (Invitrogen, ThermoFisher Scientific) were applied respectively. Neuronal-glial co-cultures were analysed under a fluorescence microscope (Olympus IX71S1F-3, USA) in 5 randomly chosen microscopic fields at 20 × magnification. Number of synaptic puncta per microscopic field was calculated using ImageJ 1.8.0 software (Schneider et al., 2012) and Synapse Counter plugin (Dzyubenko et al., 2016). Number of synaptic puncta was normalised to 100 % for untreated neurons.

2.11. Evaluation of nitric oxide concentration in cell culture medium

NO production was evaluated by the Griess method measuring nitrite level formed during spontaneous oxidation of nitric oxide in cell culture medium (Neniskyte and Brown, 2013b). NO was evaluated using a commercial Griess reagent kit and the manufacturer's (Invitrogen, ThermoFisher) provided protocol. For NO measurement, neuronal-glial co-cultures were treated with 100 nM–500 nM S100A9 for 72 h or with 100 ng/mL LPS for 72 h as positive control. Then cell culture medium was collected and centrifuged at 10000 ×*g* for 10 min.

2.12. Evaluation of TNF-α and IL-1β concentrations in cell culture medium

TNF-α and IL-1β concentrations in cell culture media were determined using commercial ELISA kits according to the manufacturer's protocols. For TNF-α assessment, neuronal-glial co-cultures were treated with 100 nM–500 nM S100A9 for 72 h. In case of IL-1β, after treatment with 500 nM S100A9 for 24 h, 3 mM bzATP (2′(3′)-O-(4-Benzoylbenzoyl)adenosine-5′-triphosphate tri(triethylammonium) salt) was added for 30 min prior to cell culture medium collection. After treatments, cell culture media were collected and centrifuged at 10000 ×*g* for 10 min at 4 °C and then stored at −20 °C.

2.13. Statistical analysis

All data are expressed as mean ± standard deviation (S.D.) with individual data plot. Experiments were replicated in at least three independent cell culture preparations. Statistical comparison between independent experimental groups was performed using a one-way ANOVA followed by LSD test (for comparison of protein densitometry results) or Tukey's test (for comparison of experimental results in primary cell cultures). Values $p < 0.05$ were considered significant. Statistical analysis was carried out using SigmaPlot (11.0 version software).

3. Results

3.1. S100A9 exerts oligomerization-state dependent neurotoxicity in neuronal-glial co-cultures

S100A9 can form various oligomeric species that may affect the activity of the protein (Gruden et al., 2016). To investigate the neurotoxicity of S100A9, we used four different protocols for preparation of recombinant S100A9 protein: freshly prepared solutions of S100A9 in PBS buffer (protocol I) or S100A9 incubated in PBS buffer at room temperature for 30 min (protocol II), 6 h (protocol III) or 24 h (protocol IV) immediately before experimental procedures. To detect the molecular mass of S100A9, indicative of oligomerization state present in different preparations, SDS gel electrophoresis under non-reductive conditions followed by Western blot analysis was performed (Fig. 1A and B). The densitometry analysis (Fig. 1B) showed that S100A9 prepared by protocol I contained very low levels of dimers, trimers and tetramers. After 30 min (protocol II), 6 h (protocol III), and 24 h (protocol IV) of incubation, the level of dimers increased substantially compared to the protocol I preparation. However, the level of dimers in the protocol III preparation was significantly higher compared to both protocols II and IV. The level of S100A9 trimers and tetramers also increased in protocol II-IV preparations compared to protocol I, but the levels of trimers and tetramers was the same in the protocol III and IV preparations. These data indicate that S100A9 prepared by protocol III contained significantly higher levels of dimers compared to the protocol I, II and IV preparations.

As different protocols for preparation of recombinant amyloidogenic proteins can result in different aggregation states with different neurotoxicity (Andrade-Talavera et al., 2022; Cizas et al., 2010), we tested whether S100A9 prepared by the four different protocols exert different neurotoxic effects in primary neuronal-glial co-cultures isolated from rat cerebellum. We used these cultures because they yield abundant neurons and glia, and they are well characterized (Bal-Price and Brown, 2001). We found these cultures to consist of 82 ± 3 % neurons ($NeuN^+$), 5 ± 2 % microglia ($Iba\text{-}1^+$/isolectin-IB_4^+) and 13 ± 3 % astrocytes ($GFAP^+$) (Supplementary Fig. 1S A). In such neuronal-glial co-cultures, S100A9 species obtained by the four different protocols exerted different

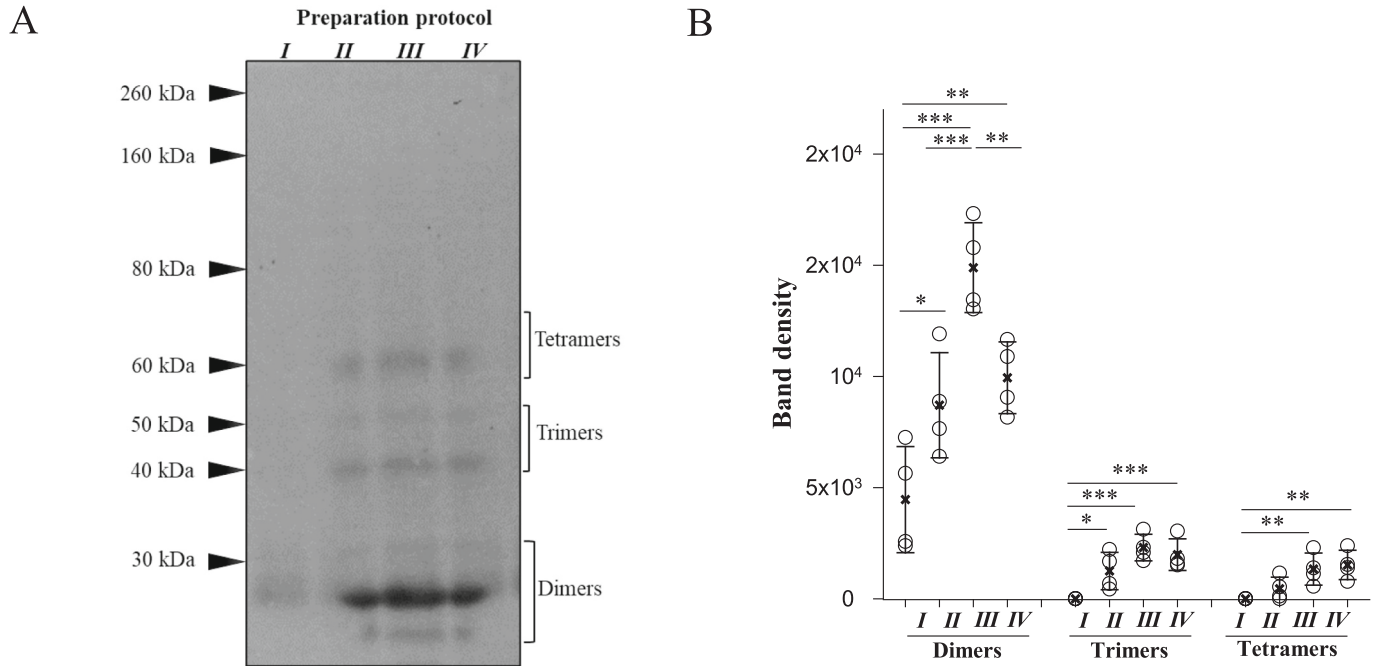

Fig. 1. Oligomerization state of S100A9 prepared by different protocols. (A) Representative image of PVDF membrane showing the molecular mass of S100A9 protein prepared by dilution with PBS buffer (protocol I), pre-incubation at room temperature for 30 min (protocol II), 6 h (protocol III) or 24 h (protocol IV). (B) Densitometric quantification of Western Blot bands. Data are presented as means ± S.D. for 4 independent experiments. The cross indicates the mean value with S.D., and each dot represents individual values of independent experiments.

neurotoxic effects at 2 μM concentrations during 48 h incubation. Fig. 2A presents representative fluorescence-microscopy images of neuronal-glial co-cultures stained with Hoechst 33342 (to detect chromatin condensation, indicative of apoptosis) and propidium iodide (to detect plasma membrane rupture, indicative of necrosis). In the untreated, control cultures, almost all neurons were viable, with no signs of apoptosis or necrosis. In cell cultures treated with S100A9 prepared by protocols I, II or IV, there was no significant increase in neuronal apoptosis or necrosis. However, treatment with S100A9 prepared by protocol III resulted in extensive neuronal cell death by apoptosis and necrosis evidenced by disrupted chromatin organization (Hoechst 33342 staining) and enhanced propidium iodide staining (Fig. 2A).

Quantitative data presented in Fig. 2B demonstrate that the S100A9 prepared by protocols I and II had no significant impact on neuronal viability: neuronal viability in control group was 96 ± 1 %, and after treatment with S100A9 prepared by protocols I and II was 88 ± 5 % and 70 ± 13 %, respectively. Neuronal numbers in these cultures were also not significantly altered and remained at 92 ± 3 % and 80 ± 10 % of the control level, respectively (Fig. 2C). In contrast, S100A9 prepared by protocol III significantly reduced neuronal viability to 15 ± 7 % (Fig. 2B), while not significantly affecting neuronal number (Fig. 2C). Lastly, S100A9 prepared by protocol IV had no statistically significant effects on neuronal viability (Fig. 2B), or neuronal number (Fig. 2C), which were 67 ± 13 % and 75 ± 11 % of the control level, respectively, although there was some neurotoxicity in some cultures (Fig. 2B).

Treatment of neuronal glial co-cultures with S100A9 prepared by protocol I increased microglial cell number by 63 ± 27 % compared to the control group (Fig. 2D). However, microglial cell count remained unchanged after treatment with S100A9 prepared by protocol II-IV.

3.2. S100A9 induces microglia-dependent neuronal loss

In the next series of experiments, we used the most toxic preparation of S100A9 (protocol III) and tested whether neurotoxicity was concentration-, time- and microglia-dependent. Neuronal-glial co-cultures were treated with 100–500 nM S100A9 for 48–72 h and then viable and dead neurons were counted. As shown in Fig. 3A, the numbers of viable, necrotic and apoptotic cells per field of view in the control neuronal-glial co-cultures were 317 ± 61, 4 ± 8 and 7 ± 5 respectively, and was not changed significantly at 100 nM or 250 nM S100A9 after 48 h incubation. However, exposure of the cultures to 500 nM S100A9 resulted in a significant decrease in viable neurons by ~30 % compared to the untreated control culture, with no significant increase in neuronal apoptosis or necrosis (Fig. 3A).

After a 72 h incubation (Fig. 3B), the numbers of viable, necrotic and apoptotic neurons per field of view in the control neuronal-glial co-cultures were 321 ± 32, 5 ± 7 and 6 ± 3 respectively. Treatment with 100 nM S100A9 had no statistically significant effect on the number of neurons. However, treatment with 250 nM S100A9 significantly reduced the number of viable neurons by about 25 % compared to the control culture, again without a notable increase in apoptosis or necrosis. 500 nM S100A9 further increased the loss of viable neurons to about 45 % compared to the control culture, without affecting the level of neuronal necrosis and apoptosis. Moreover, our data show that untreated neuronal-glial co-culture as well as S100A9-treated (100–500 nM for 72 h; preparation protocol III) express MAP2 (microtubule-associated protein 2) protein (Supplementary Fig. 3S.) indicating presence of mature neurons in these cell cultures. These results indicate that S100A9 induces a concentration-dependent loss of viable neurons in neuronal-glial co-cultures.

Interestingly, we observed that after 72 h incubation of co-cultures with 500 nM S100A9 there was a substantial increase in the number of microglial cells, as can be seen in Fig. 3D (green fluorescent cells labelled with isolectin-IB_4-AlexaFluor448 conjugate). To investigate the potential involvement of microglia in the removal of neurons from the cultures, we selectively eliminated microglia from the co-cultures with leucine methyl ester (LME, which specifically depletes microglia) and treated microglia-depleted cultures with 250–500 nM S100A9. As demonstrated in Fig. 3 C and E, in the absence of microglia there was no neuronal loss after 72 h incubation with 250 nM or 500 nM S100A9 compared to the control cultures. These findings suggest that microglia mediate the S100A9-induced neuronal loss in neuronal-glial co-cultures.

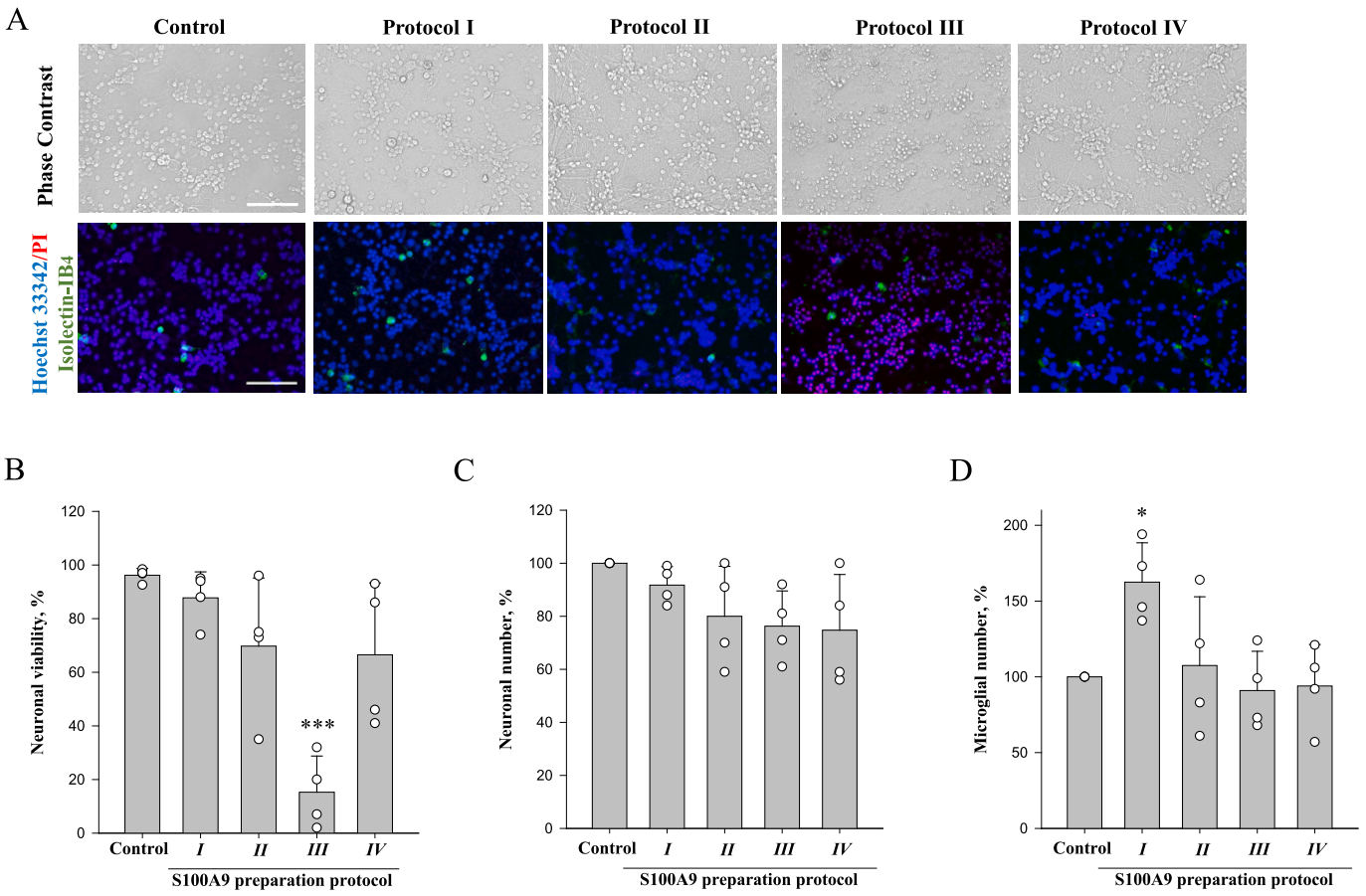

Fig. 2. The effect of 2 μM S100A9 prepared by different protocols on neuronal-glial co-cultures. (A) Representative images of control and S100A9-treated neuronal-glial co-cultures. Neuronal-glial co-cultures were incubated with 2 μM S100A9 prepared by protocols I-IV for 48 h. In phase-contrast images, neuronal cells were distinguished according to their characteristic shape and morphology. Neurons with normal chromatin structure (homogeneous Hoechst 33342 stain of nuclei) and without propidium iodide staining were considered as viable, while cells with condensed or fragmented nuclei without propidium iodide staining were considered as apoptotic. Neurons with red nuclei (propidium iodide staining) were considered necrotic. Microglial cells were labelled with isolectin IB_4-AlexaFluor488 (green). Scale bars 100 μm. Numerical data on (B) neuronal viability, (C) neuronal number and (D) microglial number. Neuronal viability is expressed as the % of all neurons that were live rather than dead (necrotic and apoptotic). The number of neurons and microglia in the S100A9-treated cultures is expressed as a percentage of the number of neurons in the untreated, control cultures. Data are presented as means ± S.D. for 4 independent experiments; $^{*}p < 0.05$, $^{***}p < 0.001$ versus untreated control. (For interpretation of the references to colour in this figure legend, the reader is referred to the web version of this article.)

We also investigated whether S100A9 exerted any effect on astrocyte numbers in the co-cultures and found that incubation with 100–500 nM S100A9 (III preparation protocol) for 48 h and 72 h did not change the total number of astrocytes (Supplementary Fig. 4S).

As the recombinant S100A9 protein was produced in *E. coli*, it is potentially contaminated with LPS endotoxin, which may activate immune cells leading to neurotoxicity in the experimental co-culture model. However, we found that the level of LPS in cell culture medium after treatment with recombinant S100A9 protein samples did not exceed 0.004 % (*w/v*), equivalent to 1.2 ng/mL. We have previously shown that 1–10 ng/mL of LPS does not cause neuronal loss in neuronal-glial co-cultures (Pampuscenko et al., 2020), suggesting that the neuronal loss observed after treatment with recombinant S100A9 protein was not due to endotoxin contamination. To further investigate the potential neurotoxic effects of residual endotoxins, we performed pre-incubation of the recombinant S100A9 protein with polymyxin B. Polymyxin B is a cationic antibiotic that binds to endotoxins and neutralizes their toxic effects (Cardoso et al., 2007). For these experiments, S100A9 was pre-incubated with 200 IU/mL polymyxin B before treatment of neuronal-glial co-cultures. Supplementary Fig. 5S shows that polymyxin B did not affect the neurotoxicity of 500 nM S100A9, suggesting that the neurotoxicity of the protein was not caused by contamination of S100A9 preparations by bacterial endotoxin.

3.3. S100A9 induces microglial activation in neuronal-glial co-cultures

Next, we investigated whether S100A9 causes microglial activation by evaluating microglial number, cell area and expression of Iba-1 (ionized calcium-binding adapter molecule 1), after exposure of co-cultures to 100–500 nM S100A9 (protocol III) for 48–72 h. As can be seen in Fig. 4A and D, there was a dose-dependent increase in microglial number in response to S100A9 treatment after 72 h, though at 48 h no significant changes in microglia numbers were observed. Treatment with 500 nM S100A9 for 72 h caused a 72 % increase in microglial number compared to the control cultures (131 ± 44 cells/field in 500 nM S100A9-treated versus 76 ± 25 cells/field in control cultures). Another marker of microglial changes - cell area, showed a tendency to increase in a concentration-dependent manner after 48 h incubation with S100A9, and a statistically significant enlargement of cell area was observed after 72 h incubation with 250 nM or 500 nM S100A9 compared to the control cultures (Fig. 4B and E). Additionally, the expression of microglial pro-inflammatory marker Iba-1 was enhanced by ~30 % after exposure to 100–500 nM S100A9 for 72 h (Fig. 4C and F). Overall, the observed changes in microglial number, morphology and Iba-1 expression suggest that addition of S100A9 induces a pro-inflammatory phenotype of microglia.

Pro-inflammatory factors produced by activated microglia may play

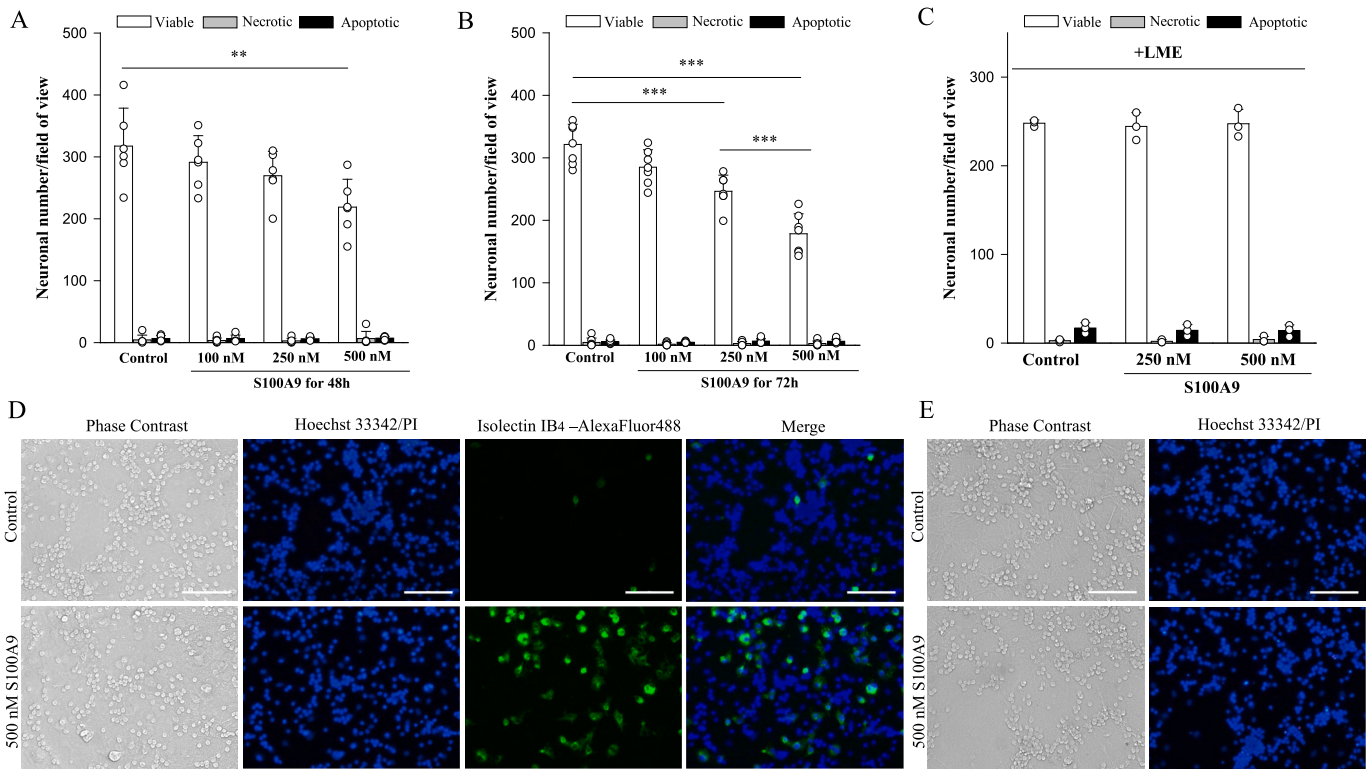

Fig. 3. S100A9 causes neuronal loss that is dependent on concentration, time and microglia. (A) and (B) – neuronal numbers in neuronal-glial co-cultures and (C) – in microglia-depleted cultures. Neuronal-glial co-cultures were incubated with S100A9 prepared by protocol III (pre-incubation at room temperature for 6 h). Cell cultures were incubated with 100–500 nM S100A9 species for 48 h (A) or 72 h (B). To deplete microglia, neuronal glial co-cultures were incubated with L-leucine methyl ester (LME), and these microglia-depleted cultures were then exposed to 250–500 nM S100A9 (protocol III) for 72 h. Neurons with homogeneously Hoechst 33342-stained nuclei were considered as viable; neurons with condensed or fragmented nuclei as apoptotic, and propidium iodide positive neurons were considered necrotic. Data are presented as means ± S.D. for 3–7 independent experiments; $^{**}p < 0.01$, $^{***}p < 0.001$. Representative images of control and S100A9 treated (D) neuronal-glial co-cultures and (E) microglia-depleted cultures. Microglial cells were labelled with isolectin IB_4-AlexaFluor488 (green). Scale bars 100 μm. (For interpretation of the references to colour in this figure legend, the reader is referred to the web version of this article.)

an important role in mediating neuronal damage. Thus, we investigated the effect of S100A9 on production of TNF-α, IL-1β and nitric oxide (NO) in neuronal-glial co-cultures. The levels of the pro-inflammatory cytokine TNF-α in the cultures 72 h after treatment with 0, 100, 250 and 500 nM S100A9 were: 63 ± 22, 90 ± 32, 146 ± 54 and 171 ± 53 pg/mL, respectively (Fig. 5A).

We found that the level of IL-1β in control cultures, and cultures treated with 500 nM S100A9 for 24 h, were below the detection limit (<32 pg/mL) (Fig. 5B). However, the release of expressed IL-1β normally requires a separate releasing stimulus (such as bzATP), and we found that stimulation of 500 nM S100A9-primed cells with 3 mM bzATP for 30 min resulted in the release of IL-1β into the cell culture medium: after such treatment the IL-1β concentration increased to 87 ± 18 pg/mL, suggesting that S100A9 induced the expression and/or intracellular maturation of IL-1β.

In contrast to the pro-inflammatory cytokines, we did not observe any significant changes in NO production following S100A9 treatment for 72 h (Fig. 5C): the level of NO (measured as nitrite) in control culture was 2.4 ± 0.7 μM and after treatment with 100–500 nM S100A9 it remained unchanged. In comparison, 100 ng/ml LPS, which was used as a positive control, caused a significant elevation of NO to 24 ± 9 μM after 72 h incubation.

Altogether, these results suggest that S100A9 induces a mild, pro-inflammatory activation of microglia.

3.4. S100A9 induces phosphatidylserine exposure in neuronal-glial co-cultures

Phosphatidylserine exposure on the cell surface serves as an "eat-me" signal for the phagocytosis of stressed or dying cells by phagocytic cells, including the phagocytosis of neurons by microglia (Butler et al., 2021). Therefore, we investigated the effect of 100–500 nM S100A9 (protocol III) on the phosphatidylserine exposure on neuronal cells using Annexin V-Cy3 staining. In Fig. 6A, representative images of phosphatidylserine exposure are presented: untreated control neuronal-glial co-cultures exhibited minimal Annexin V fluorescence (red colour), however, cell cultures exposed to S100A9 showed a marked increase in Annexin V fluorescence intensity, indicating enhanced phosphatidylserine exposure. Quantitative data are presented in Fig. 6B, demonstrating that treatment with 100 nM S100A9 for 72 h increased Annexin V fluorescence intensity by 20 ± 7 %, 250 nM S100A9 increased fluorescence by 39 ± 8 % and 500 nM S100A9 increased fluorescence by 63 ± 13 % compared to control co-cultures. Thus, S100A9 appears to increase the exposure of phosphatidylserine by neurons, despite no significant apoptosis or necrosis, probably as a result of neuronal stress (Neher et al., 2011).

To elucidate the specific role of glial cells in this process, we evaluated phosphatidylserine exposure in pure neuronal cultures obtained by Ara-C treatment (which depletes both microglia and astrocytes). S100A9 had no effect on phosphatidylserine exposure in pure neuronal cultures (Fig. 6C). These data suggest that glial cells mediate S100A9-induced phosphatidylserine exposure on neurons, potentially thereby promoting microglial phagocytosis of such neurons.

Phosphatidylserine can be exposed reversibly on the cell surface of live cells in response to some type of stress or irreversibly on apoptotic cells because of caspase-3 activation (Butler et al., 2021). To investigate whether caspase-3 is involved in S100A9-unduced phosphatidylserine exposure, we used a transwell system for neuronal and microglial cell

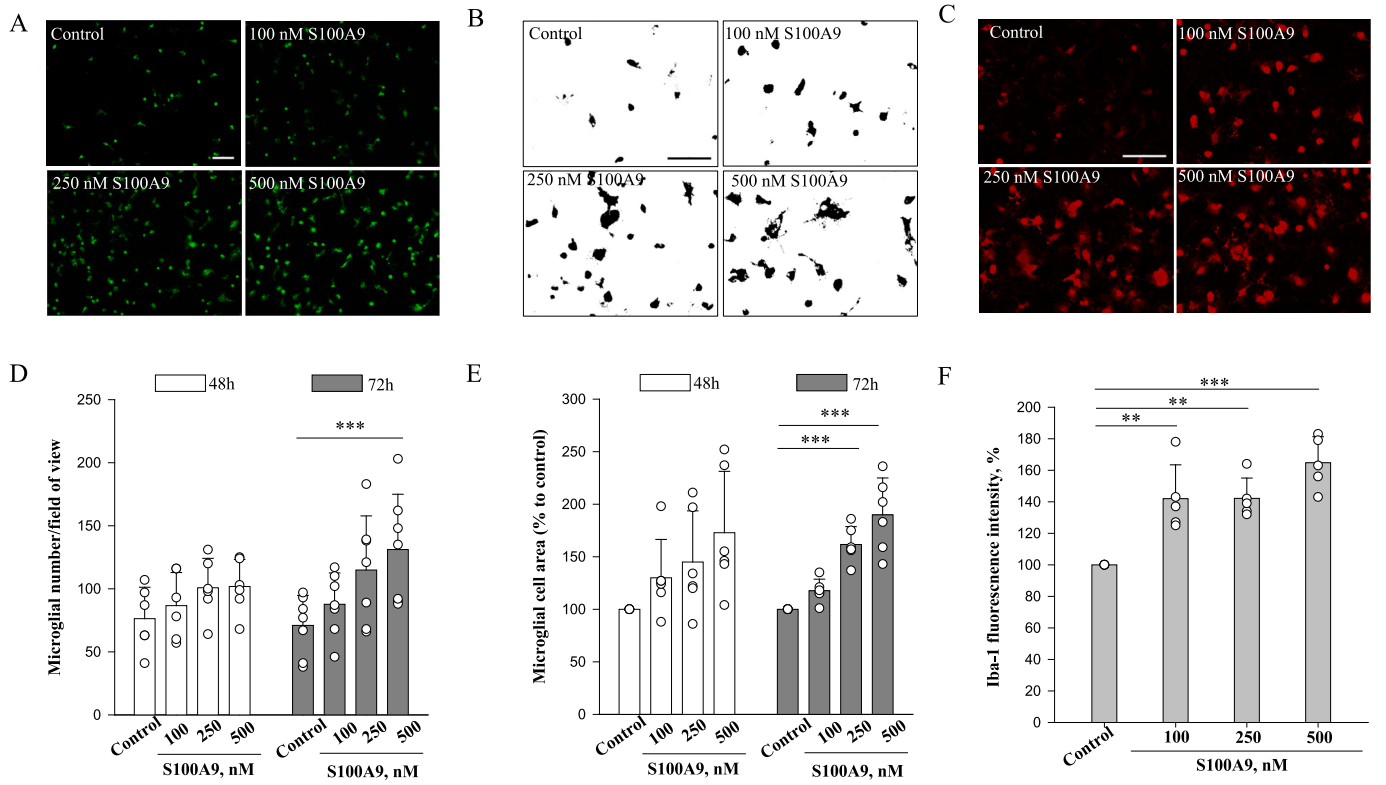

Fig. 4. The effects of S100A9 on microglia in neuronal-glial co-cultures. Representative images of (A) – isolectin IB_4-AlexaFluor488 (green) labelled microglial cells, (B) –binary images obtained after processing the fluorescence images of isolectin IB_4-AlexaFluor488 staining to estimate microglial cell area, and (C) – Iba-1 immunostaining (red). Scale bars 100 μm. Numerical data on (D) – microglial number, (E) – microglial cell area and (F) – Iba-1 fluorescence intensity. Neuronal-glial co-cultures were incubated with S100A9 prepared by protocol III (pre-incubation at room temperature for 6 h). For microglial number and cell area analysis, cell cultures were treated with 100–500 nM S100A9 (prepared by protocol III) for 48 h and 72 h, for Iba-1 analysis – for 72 h. Data are presented as means ± S.D. for 3–7 independent experiments; $^{**}p < 0.01$, $^{***}p < 0.001$. (For interpretation of the references to colour in this figure legend, the reader is referred to the web version of this article.)

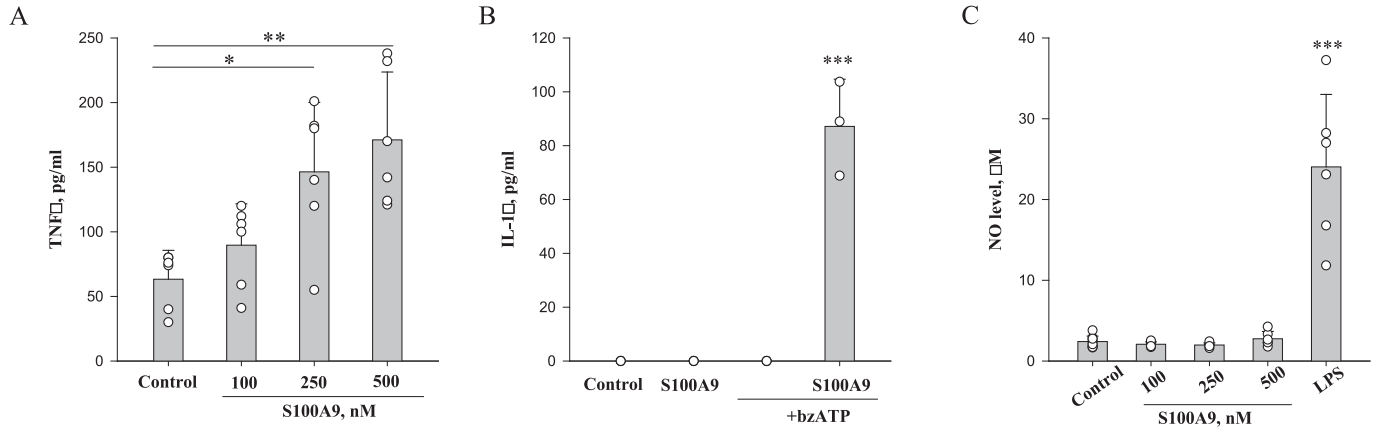

Fig. 5. S100A9 induces production of pro-inflammatory factors. Level of (A) – TNF-α, (B) – IL-1β and (C) – nitric oxide (NO). For (A) and (C), neuronal-glial co-cultures were incubated with 100–500 nM S100A9 (prepared protocol III) or 100 ng/ml LPS (positive control) for 72 h. For (B), cell culture exposure to 500 nM S100A9 (prepared by protocol III) for 24 h was followed by 3 mM bzATP treatment for 1 h. Data are presented as means ± S.D. for 4 independent experiments; $^{*}p < 0.05$, $^{**}p < 0.01$ ***, $p < 0.001$ versus untreated control.

co-culturing (Supplementary Fig. 6S and 7S). After treatment with 500 nM S100A9 neuronal cell layer was analysed for caspase-3 levels by Western Blot method. Our results indicate that caspase-3 (band between 15 and 25 kDa) was present in both the control group and S100A9 protein-treated group, with no statistically significant difference observed between these two groups. These data suggest that S100A9-induced phosphatidylserine exposure occurred in caspase-3 independent manner.

3.5. S100A9 enhances microglial phagocytic activity in monocultures and neuronal-glial co-cultures

To investigate the effects of S100A9 on phagocytic activity, we evaluated the capacity of microglia to engulf fluorescent beads that were carboxylate modified to mimic the negative charge of phosphatidylserine. Microglial cell monocultures were exposed to 100–500 nM S100A9 (protocol III preparation) for 24 h, then fluorescent beads were added

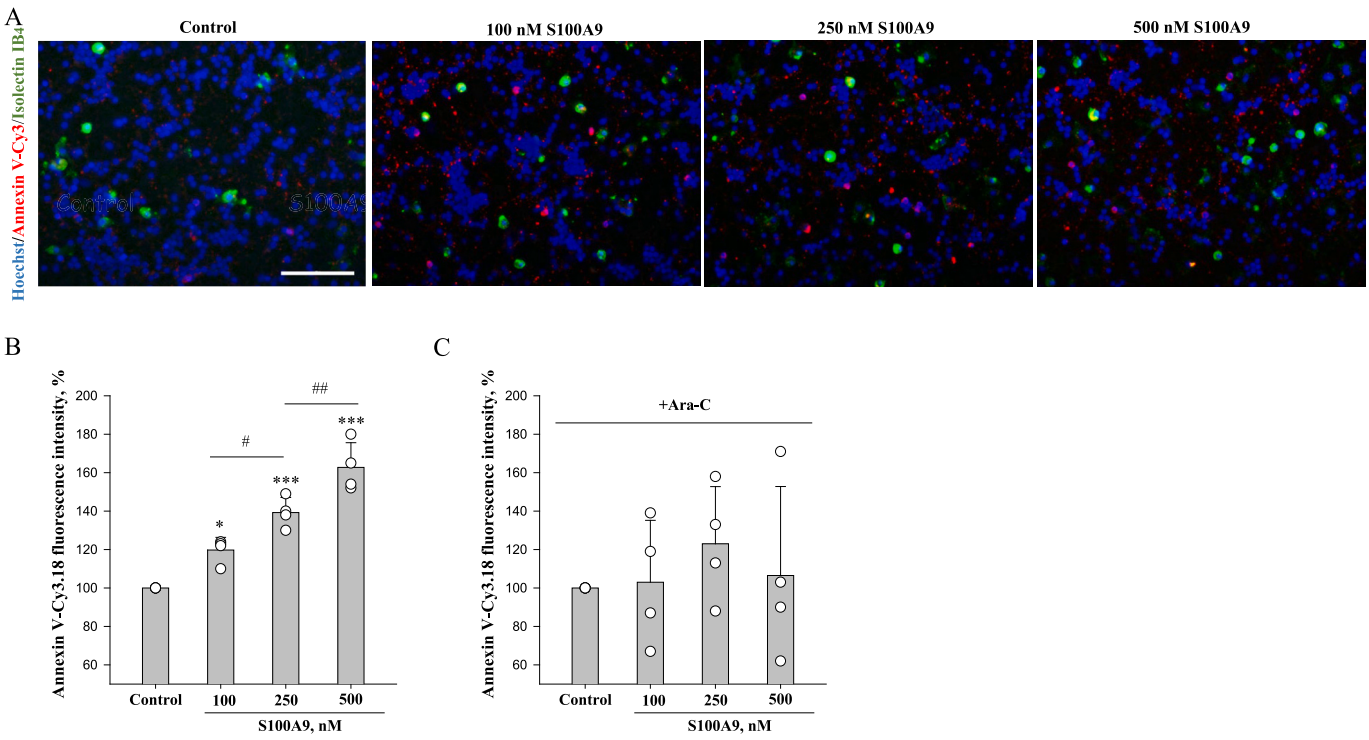

Fig. 6. S100A9 induces phosphatidylserine exposure in neuronal-glial co cultures. (A) Representative images of control and S100A9-treated neuronal-glial co-cultures stained with Annexin V- Cy3 (red, binding to exposed phosphatidylserine), Hoechst 33342 (blue, cell nuclei) and isolectin IB_4-AlexaFluor488 (green, microglia). Scale bars 100 μm. Annexin V- Cy3 fluorescence intensity in (B) neuronal-glial co-cultures and (C) in pure neuronal cell cultures. Cell cultures were treated with 100–500 nM S100A9 (prepared by protocol III) for 72 h. Pure neuronal cell cultures were obtained by cytosine β- D–arabinofuranoside (Ara—C) treatment. Changes in AnnexinV-Cy3 fluorescence intensity after S100A9 treatment were expressed as a percentage of the fluorescence intensity in the untreated control cultures. Data are presented as means ± S.D. for 4–5 independent experiments; *$p < 0.05$, ***$p < 0.001$ versus untreated control and # $p < 0.05$, ## $p < 0.01$ versus appropriate S100A9 treated groups. (For interpretation of the references to colour in this figure legend, the reader is referred to the web version of this article.)

and the numbers of phagocytosed beads were evaluated after 2 h (representative images are presented in Fig. 7A). Quantitative data presented in Fig. 7 B and C show that microglial cells phagocytosed on average 4 ± 2 fluorescent beads per cell in the untreated control culture. S100A9 strongly increased this phagocytosis to 15 beads per cell in the case of 500 nM S100A9, and 100 nM and 250 nM S100A9 increased phagocytic activity similarly. However, 100 nM and 250 nM S100A9 did not affect the total number of phagocytic microglia compared to the control group in which the number of phagocytic microglia was 61 ± 18 % (i.e. 61 % of the microglia had one or more beads within them, Fig. 7 C). Only 500 nM S100A9 significantly increased the proportion of microglia phagocytosing beads, by 28 ± 11 % (Fig. 7 C).

To further assess phagocytosis in response to S100A9, we measured the expression of CD68 protein, a lysosomal glycoprotein commonly associated with phagocytosis in myeloid cells (including microglia). Neuronal-glial co-cultures were treated with 100–500 nM S100A9 (preparation protocol III) for 72 h and then CD68 expression was analysed by immunofluorescence staining. Results presented in Fig. 7 D show that 100–500 nM S100A9 treatment increased CD68 fluorescence intensity by ~20–25 % indicating upregulated phagocytic processes in neuronal-glial co-cultures.

Overall, these results indicate that 100–500 nM S100A9 substantially increased the phagocytic capacity of microglia in pure cultures and neuronal-glial co-cultures.

3.6. Nanomolar S100A9 induces synaptic loss in neuronal-glial co-cultures

Progressive loss of synapses occurs before neuronal loss during neurodegenerative diseases, and can contribute to the pathology and brain dysfunction (Wilson et al., 2023). To determine whether S100A9 affects synaptic density, neuronal-glial co-cultures were treated for 72 h with 0, 10 or 100 nM S100A9 (protocol III preparation), i.e. at concentrations of S100A9 that do not cause significant neuronal loss. Synaptic density was analysed by immunostaining using antibodies against pre-synaptic (synapsin-1) and post-synaptic (PSD-95) proteins, and the co-localization of these markers was used as a measure of synaptic puncta. As can be seen from Fig. 8A, after image processing synapsin-1 (green) and PSD-95 (red) antibodies stain puncta within the culture, and most of these puncta colocalize at what are presumably functional synapses (yellow). Fig. 8B shows that the density of these synapses within the cultures was reduced significantly by ~20 % after treatment with 10 nM and 100 nM S100A9 compared to the untreated control cultures (for which synaptic density was normalised to 100 %). To assess whether S100A9-induced synaptic loss was microglia-dependent, we analysed synaptic densities in microglia-depleted cultures. Fig. 8B shows that after microglial cell elimination by LME treatment, 10–100 nM S100A9 had no effect on synaptic density suggesting that S100A9 causes synaptic loss through microglial phagocytosis. We also found that S100A9 stimulates phagocytosis of synaptosomes (isolated synapses) by microglial cells in pure cell cultures (Supplementary Fig. 8S). These data support our hypothesis that S100A9 protein promotes synapse loss through enhanced phagocytosis.

Altogether, these findings indicate that S100A9 can cause synaptic loss in neuronal-glial co-cultures at low nanomolar concentrations.

4. Discussion

The pro-inflammatory protein S100A9 is gaining attention for its potential deleterious role in neurodegenerative processes (Cristóvaõ and Gomes, 2019). S100A9 was found to contribute to the memory impairment and neuropathology in transgenic animal models of AD (Chang

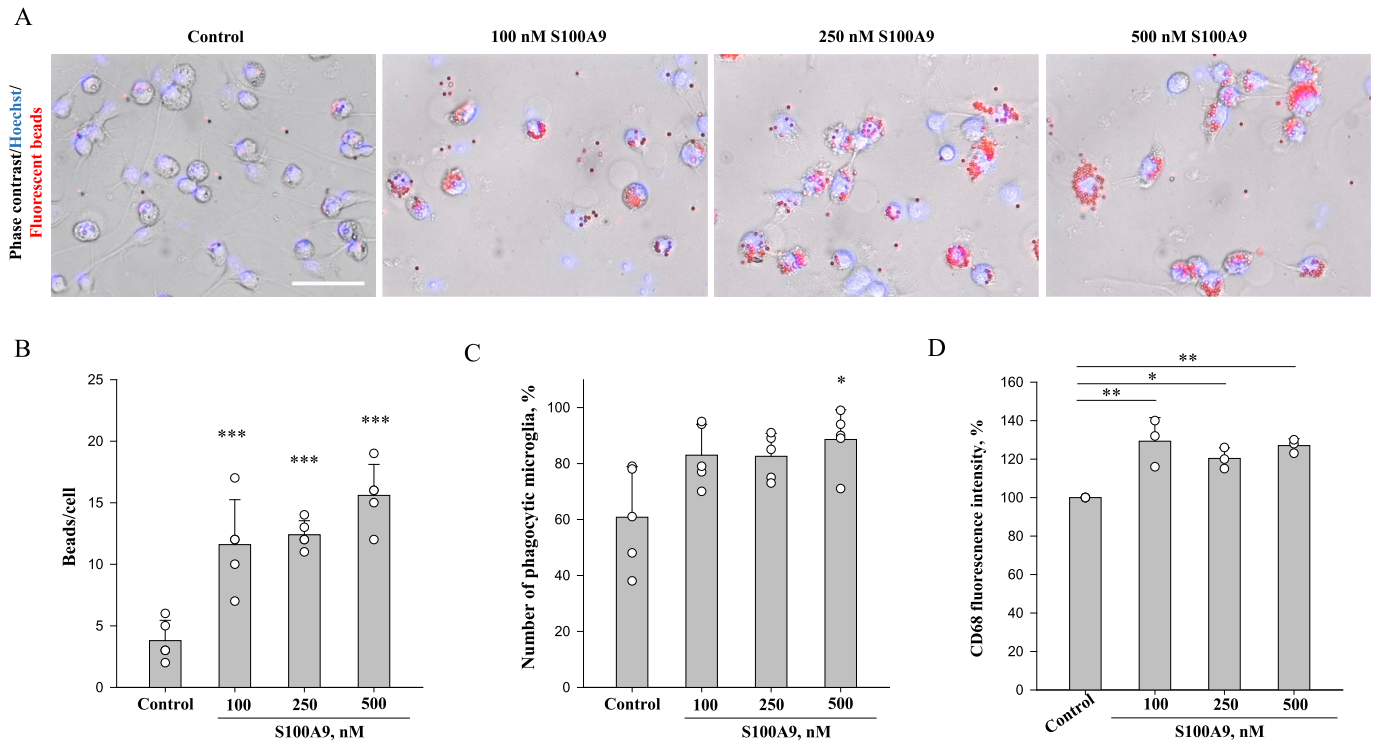

Fig. 7. S100A9 stimulates microglial phagocytic activity. (A) Representative images of control and S100A9-treated pure microglial cell cultures phagocytosing carboxylate-modified 2 μm latex beads (red). Cell nuclei was labelled with Hoechst 33342. Scale bars 100 μm. (B) Number of beads within microglial cells and (C) number of phagocytic microglia. Pure microglial cell cultures were treated with 100–500 nM S100A9 (prepared by protocol III) for 24 h. (D) CD68 fluorescence intensity in neuronal-glial co-cultures treated with S100A9 (protocol III) for 72 h. Changes in CD68 fluorescence intensity after S100A9 treatment were expressed as a percentage of the fluorescence intensity in the untreated control cultures. Data are presented as means ± S.D. for 3–5 independent experiments; *p < 0.05, **p < 0.01, ***p < 0.001 versus untreated control. (For interpretation of the references to colour in this figure legend, the reader is referred to the web version of this article.)

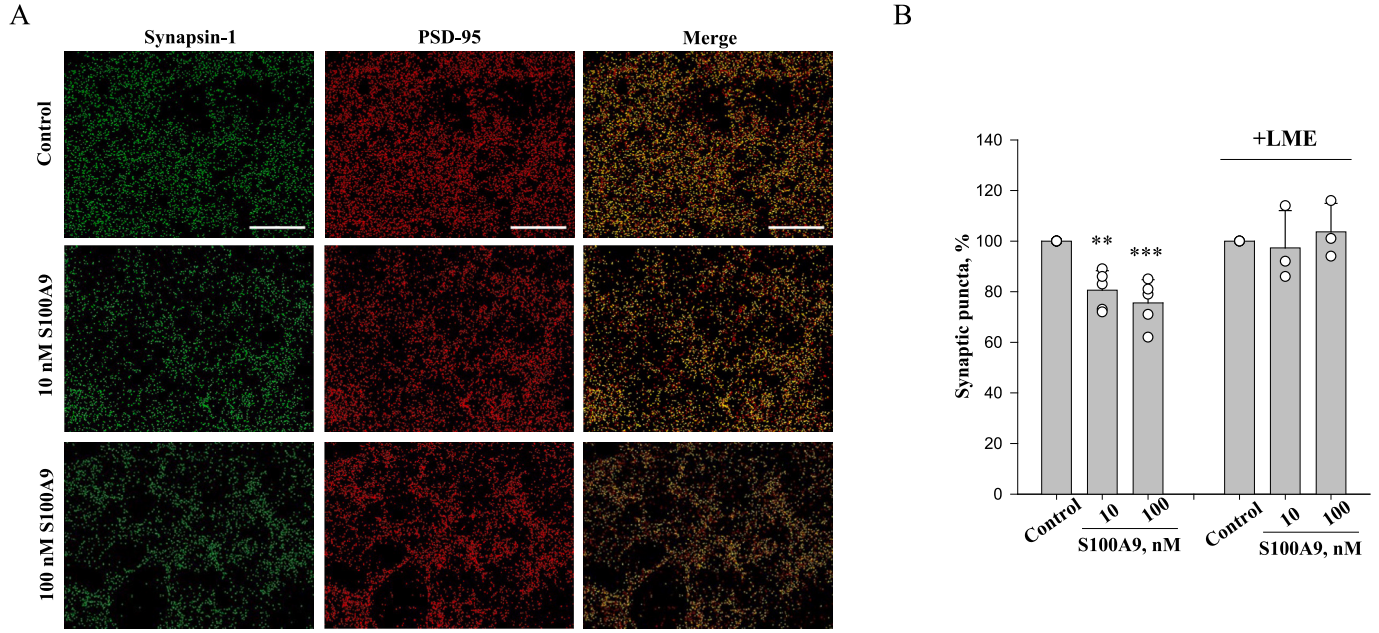

Fig. 8. S100A9 induces synaptic loss in neuronal-glial co-cultures. (A) Representative images of synaptic puncta density obtained using ImageJ 1.8.0 software and Synapse Counter plugin after immunostaining for synapsin-1 and PSD-95 proteins. Synapsin-1 (green) and PSD-95 (red) represent individual pre-synaptic and post-synaptic sites. Colocalization between synapsin-1 and PSD-95 (yellow) indicates synaptic puncta. Scale bars 100 μm. (B) Statistical data on synaptic puncta density. Neuronal-glial co-cultures were treated with 10 and 100 nM S100A9 (prepared by protocol III) for 72 h. To deplete microglia, neuronal glial co-cultures were incubated with L-leucine methyl ester (LME). The number of synaptic puncta in S100A9-treated cultures is expressed as a percentage of synaptic puncta in the untreated control cultures. Data are presented as means ± S.D. for 3–5 independent experiments; **p < 0.01, ***p < 0.001 versus untreated control. (For interpretation of the references to colour in this figure legend, the reader is referred to the web version of this article.)

et al., 2012; Kim et al., 2014), and intranasal injections of S100A9 induced memory deficits in mice (Gruden et al., 2016). The progressive brain dysfunction characteristic of neurodegenerative diseases is probably in part caused by the progressive loss of synapses and neurons, but the molecular pathways responsible for this loss of synapses and neurons remain largely unclear (Wilson et al., 2023). Cell death by phagocytosis is considered to be one of the means by which neurons die during neurodegeneration (Butler et al., 2021; Fricker et al., 2018). This type of neuronal death can be provoked by exposure of "eat-me" signals on stressed-but-viable cells, causing their subsequent phagocytosis by inflamed microglia (Neher et al., 2011; Brown, 2024). In this study, we show for the first time that S100A9 at nanomolar concentrations causes neuronal loss by activating microglia to phagocytose stressed neurons (Fig. 9, graphical abstract). This hypothesis is supported by several lines of evidence, including (i) S100A9 induced neuronal exposure of the "eat-me" signal phosphatidylserine during neuronal loss in the absence of apoptosis and necrosis, (ii) S100A9 stimulated microglial phagocytosis of phosphatidylserine-mimicking beads, and (iii) S100A9-induced neuronal loss was prevented by depleting microglia from the neuronal-glial cultures. Phagocytosis of stressed-but-viable neurons occurs when neurons have been stressed sufficiently to induce signalling for phagocytosis, but not sufficiently to induce neuronal death directly, and when microglial phagocytosis has been activated (Butler et al., 2021).

Synaptic loss occurs prior to neuronal loss in many neurodegenerative diseases (Wilson et al., 2023). In this study, we demonstrate that S100A9 is capable of inducing synaptic loss in neuronal-glial co-cultures. Notably, synaptic loss occurred at concentrations lower than those required for neuronal body loss: neuronal loss in cell cultures occurred at 250–500 nM, while synaptic loss occurred at 10–100 nM. However, 100 nM S100A9 was able to induce neuronal phosphatidylserine exposure, suggesting that exposure of phosphatidylserine on the surface of synapses or neurons may serve as a signal for phagocytosis of synapses and neuronal bodies. In earlier studies, phosphatidylserine exposure was considered as an apoptotic marker, but there is now substantial evidence that live cells can also expose phosphatidylserine, triggered for example by an elevation of cytosolic calcium (Shin and Takatsu, 2020; Shlomovitz et al., 2019; Suzuki et al., 2010). Neuronal phosphatidylserine exposure can be triggered by sub-toxic levels of glutamate, oxidants or activated microglia, but is reversible on viable neurons if the trigger is removed; however, if activated microglia are present during neuronal phosphatidylserine exposure, then such neurons are phagocytosed, resulting in neuronal death (Neher et al., 2011; Neher et al., 2013). Moreover, local phosphatidylserine externalization on synapses mediates synaptic elimination by microglia not only during development (Scott-Hewitt et al., 2020), but also during pathology (Rueda-Carrasco et al., 2023). Thus, the synaptic loss induced by S100A9 might be due to microglial phagocytosis of phosphatidylserine-exposing synapses.

We showed here that low nanomolar levels of S100A9 induced synapse loss in cell cultures, high nanomolar levels of S100A9 induced neuronal loss, apparently by microglial phagocytosis, while micromolar levels of S100A9 induced neuronal necrosis. Notably, micromolar levels of S100A9 had no effect on total neuronal number suggesting that microglial clearance of dead cells can be impacted by high concentration of toxic S100A9 species. Similarly, S100A9 was found to affect BV-2 cell phagocytosis in a dose-dependent manner: low levels of S100A9 stimulated microglial phagocytosis, while high levels reduced phagocytic capacity (Zhang et al., 2023a, 2023b). Overall, our data suggests that S100A9 induces neuronal stress that causes direct neuronal death at high levels of S100A9, but induces microglial phagocytosis of stressed-but-viable synapses or neurons at low levels of S100A9. This raises the question of what levels of S100A9 are found extracellularly in the brain during neurodegeneration? S100A9 is a relatively abundant protein, for example constituting 45 % of cytosolic protein in neutrophils, and is released by myeloid cells in inflammatory conditions (Wang et al., 2018a, 2018b). S100A9 expression is increased in microglia during neurodegeneration (Shepherd et al., 2006) and is increased in the brain tissue of AD patients (Kummer et al., 2012). Soluble S100A9 was found to decline from 0.8 nM in controls to 0.4 nM in the CSF of AD patients (Horvath et al., 2016), while aggregated forms of S100A9 increased in AD brain tissue (Shepherd et al., 2006). S100A9 can aggregate into amyloidogenic structures in a similar way as Aβ (Wang et al., 2014), so the reduction of CSF levels of S100A9 during AD may correspond to soluble S100A9 aggregating (or S100A9 changing to a conformation not recognized by the anti-S100A9 antibodies). These levels of soluble S100A9 measured in CSF suggest that it is feasible that S100A9 could be present in extracellular brain tissue at low nanomolar levels.

In the context of neurodegenerative diseases, microglia can be morphologically and functionally activated, and this may contribute to neuronal damage (Fricker et al., 2018). Our experimental findings demonstrate that neuronal loss in S100A9 treated co-cultures was accompanied by microglial changes indicated by their number increase, soma enlargement, upregulated Iba-1 expression and pro-inflammatory cytokine (TNF-α and IL-1β) production. S100A9 is itself a pro-inflammatory protein that can bind and activate TLR4 and RAGE receptors (Wang et al., 2018a, 2018b). Activation of these receptors was

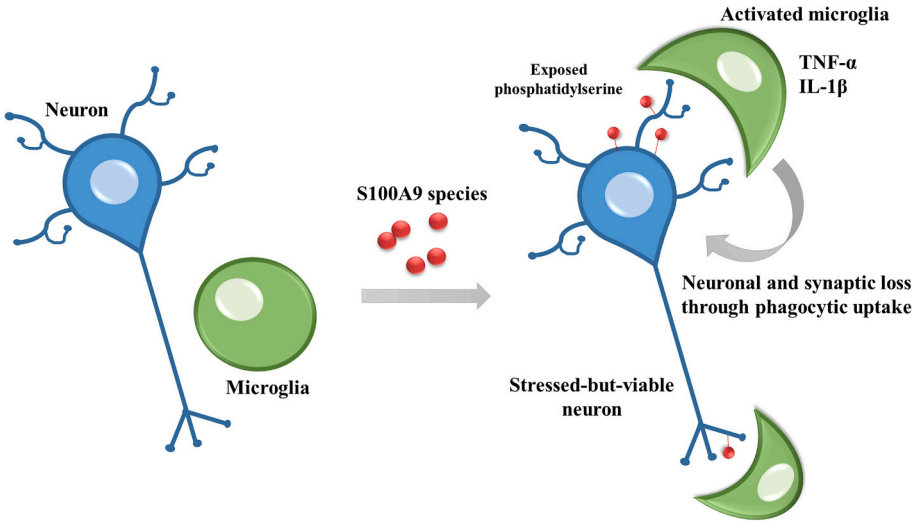

Fig. 9. Graphical abstract. S100A9 protein species induce microglial activation and phosphatidylserine exposure on the outer leaflet of neuronal membranes leading to microglial phagocytosis of stressed synapses and neurons.

found to trigger downstream signalling pathways, including activation of NF-κB, leading to the production of pro-inflammatory cytokines in microglial BV-2 cell line, as well as reorganization of the cytoskeleton (Wang et al., 2018a, 2018b). We have recently shown that microglial activation via TLR4 and caspase-1 pathway in response to tau protein caused neuronal loss through phagocytic uptake (Pampuscenko et al., 2023). Moreover, TNF-α itself can induce phosphatidylserine exposure on neuronal cells and subsequent elimination by microglia (Neniskyte et al., 2014). Furthermore, activation of microglia can trigger the upregulation of phagocytic receptors and signalling pathways, allowing microglia to recognize and engulf stressed neurons (Butler et al., 2021). Understanding the molecular mechanism of S100A9-induced synaptic and neuronal loss could help to prevent it. Therefore, it is important to further elucidate the precise mechanisms of S100A9-mediated neurotoxicity that may be potential therapeutic targets to prevent neurodegeneration.

Changes in the accumulation of misfolded proteins and their aggregation is thought to initiate neurodegenerative processes through disruption of normal cellular functions, leading to a wide range of consequences, including neuronal cell death and inflammation (Wilson et al., 2023). Aggregation-state dependent neurotoxicity was shown by Gruden et al., 2016 demonstrating the ability of oligomers and fibrils of S100A9 (but not the native form) to induce neurochemical remodelling and initiate memory deficits in mice. Here, we show that a S100A9 protein preparation containing oligomeric forms exerts neurotoxic effects through inflammatory processes. S100A9 may aggregate itself or with other proteins, resulting in different cellular effects. For example, the S100A8/S100A9 heterodimer was found to strongly activate phagocytes, while S100A8/S100A9 tetramers blocked the TLR4-binding site and interacted with the CD69 receptor leading to inflammation resolution (Russo et al., 2022). Indeed, the presence of monomeric, soluble aggregates of S100A9, and insoluble S100A9 species in AD brain homogenates (Shepherd et al., 2006) suggests that pathology might be associated with S100A9 of various conformations. S100A9 has also been found in senile plaques in association with Aβ and in the surrounding regions where Aβ is not present (Wang et al., 2014), implying that S100A9 appears in the extracellular space in a free form and may alter physiological brain processes from outside the cell. Importantly, S100A9 tends to form heterocomplexes with S100A8, but S100A8-positive plaques are not present in the hippocampus, dental gyrus, or neocortical areas where S100A9-positive plaques are observed (Wang et al., 2014). The source of S100A9 in brain tissue remains unclear, however, it has been shown to increase and aggregate as a consequence of age, ischemic/haemorrhagic damage or traumatic brain injury (Swindell et al., 2013; Wang et al., 2018a, 2018b; Wang et al., 2024; Ziegler et al., 2009). During aging, brain ischemia and subarachnoid haemorrhage, S100A9 has been found to be upregulated in microglial cells (Swindell et al., 2013; Wang et al., 2024; Ziegler et al., 2009) suggesting it may contribute to the inflammatory response and subsequent tissue damage. In a murine model of traumatic brain injury, S100A9 quickly forms intracellular and extracellular aggregates and can be produced by both neuronal and microglial cells (Wang et al., 2018a, 2018b). Overall, these data suggest that under certain pathophysiological conditions, S100A9 can be present in the brain tissue in different aggregation states, both inside and outside cells, initiating pathological cascades that lead to neurodegeneration.

In our study, the neurotoxic effect of extracellular S100A9 species was closely linked to microglial activation and enhanced phagocytic activity. Emerging evidence supports the hypothesis that inflamed microglia and disrupted phagocytic processes contributes to neurodegeneration progression. Post-mortem examination of the brains of individuals with AD and PD has found an increase in phagocytic (CD68-positive) microglia (Croisier et al., 2005; Hopperton et al., 2017; Kouli et al., 2020; Minett et al., 2016) and up-regulation of genes for phagocytosis (Podleśny-Drabiniok et al., 2020; Tremblay et al., 2019), indicating disrupted phagocytic processes. This is further supported by increased galectin-3 (García-Revilla et al., 2022) and C3/C1q (Chatterjee et al., 2023; Wu et al., 2019) in CSF or brain tissue, which bind to exposed phosphatidylserine and act as neuronal opsonins, triggering their subsequent engulfment (Butler et al., 2021). In experimental models, excessive microglial phagocytosis of neurons and synapses was found to occur in response to pathological factors related to AD and PD pathology, such as LPS (Dundee et al., 2023; Neher et al., 2011), Aβ (Neniskyte et al., 2011), and tau protein (Brelstaff et al., 2018; Pampuscenko et al., 2020, 2021), which induced reversible exposure of phosphatidylserine on live neurons, and subsequent phagocytosis by microglia. Furthermore, microglia have been observed to phagocytose viable dopaminergic neurons, leading to motor dysfunction and a shortened lifespan in *Drosophila* overexpressing phagocytic receptors (Hakim-Mishnaevski et al., 2019). Specific loss of dopaminergic neurons in the *substantia nigra* also occurred through microglial phagocytosis in an inflammatory model of PD (Milde et al., 2021). Our data indicate that S100A9 may also contribute to neurodegeneration through inducing microglial phagocytosis of stressed neurons.

Current study provides valuable insights into the mechanisms of cell death related to S100A9-induced neuroinflammatory conditions, however, several limitations must be acknowledged. Our findings are based on in vitro models, which are useful for understanding cellular and molecular processes, but do not fully replicate the complexity of in vivo conditions. Another important limitation is that the study did not analyze different neuronal populations and their interaction with microglia as well as astrocytes under different conditions. Future research should focus on investigating specific neuronal subtypes and brain regions to better understand the role of S100A9 in the pathogenesis of neurodegenerative disorders. Moreover, more precise tools should be used to quantify microglial proliferation and to identify synaptic material or live neurons engulfed by microglia to better understand mechanisms of neuronal loss during neurodegeneration.

5. Conclusion

Our findings suggest that microglial inflammatory activation contributes to the loss of synapses and neurons in response to extracellular S100A9 protein.

Funding

This work has received funding from the Research Council of Lithuania (LMTLT), agreement No S-MIP-23-98 (APNEVIR).

CRediT authorship contribution statement

Katryna Pampuscenko: Writing – original draft, Visualization, Supervision, Methodology, Investigation, Funding acquisition, Formal analysis, Data curation. **Silvija Jankeviciute:** Writing – review & editing, Methodology, Investigation, Formal analysis, Data curation. **Ramune Morkuniene:** Writing – review & editing, Methodology, Formal analysis. **Darius Sulskis:** Writing – review & editing, Methodology, Investigation, Formal analysis. **Vytautas Smirnovas:** Writing – review & editing, Methodology. **Guy C. Brown:** Writing – review & editing, Conceptualization. **Vilmante Borutaite:** Writing – review & editing, Supervision, Conceptualization.

Declaration of competing interest

Nothing to disclose.

Appendix A. Supplementary data

Supplementary data to this article can be found online at https://doi.org/10.1016/j.nbd.2025.106817.

Data availability

Data will be made available on request.

References

Andrade-Talavera, Y., Chen, G., Pansieri, J., Arroyo-García, L.E., Toleikis, Z., Smirnovas, V., Johansson, J., Morozova-Roche, L., Fisahn, A., 2022. S100A9 amyloid growth and S100A9 fibril-induced impairment of gamma oscillations in area CA3 of mouse hippocampus ex vivo is prevented by Bri2 BRICHOS. Prog. Neurobiol. 219, 102366. https://doi.org/10.1016/J.PNEUROBIO.2022.102366.

Asher, S., Priefer, R., 2022. Alzheimer's disease failed clinical trials. Life Sci. 306, 120861. https://doi.org/10.1016/J.LFS.2022.120861.

Bal-Price, A., Brown, G.C., 2001. Inflammatory neurodegeneration mediated by nitric oxide from activated glia-inhibiting neuronal respiration, causing glutamate release and excitotoxicity. J. Neurosci. 21, 6480–6491. https://doi.org/10.1523/JNEUROSCI.21-17-06480.2001.

Bartels, T., De Schepper, S., Hong, S., 2020. Microglia modulate neurodegeneration in Alzheimer's and Parkinson's diseases. Science 370, 66–69. https://doi.org/10.1126/science.abb8587.

Brelstaff, J., Tolkovsky, A.M., Ghetti, B., Goedert, M., Spillantini, M.G., 2018. Living neurons with tau filaments aberrantly expose phosphatidylserine and are phagocytosed by microglia. Cell Rep. 24, 1939–1948 e4. https://doi.org/10.1016/j.celrep.2018.07.072.

Brown, G.C., 2021. Neuronal loss after stroke due to microglial phagocytosis of stressed neurons. Int. J. Mol. Sci. 22, 13442. https://doi.org/10.3390/IJMS222413442.

Brown, G.C., 2024. Cell death by phagocytosis. Nat. Rev. Immunol. 24, 91–102. https://doi.org/10.1038/S41577-023-00921-6.

Butler, C.A., Popescu, A.S., Kitchener, E.J.A., Allendorf, D.H., Puigdellivol, M., Brown, G. C., 2021. Microglial phagocytosis of neurons in neurodegeneration, and its regulation. J. Neurochem. 158, 621–639. https://doi.org/10.1111/JNC.15327.

Cardoso, L.S., Araujo, M.I., Góes, A.M., Pacífico, L.G., Oliveira, R.R., Oliveira, S.C., 2007. Polymyxin B as inhibitor of LPS contamination of Schistosoma mansoni recombinant proteins in human cytokine analysis. Microb. Cell Factories 6, 1–6. https://doi.org/10.1186/1475-2859-6-1.

Chang, K.A., Kim, H.J., Suh, Y.H., 2012. The role of S100a9 in the pathogenesis of Alzheimer's disease: the therapeutic effects of S100a9 knockdown or knockout. Neurodegener. Dis. 10, 27–29. https://doi.org/10.1159/000333781.

Chatterjee, M., Özdemir, S., Kunadt, M., Koel-Simmelink, M., Boiten, W., Piepkorn, L., Pham, T.V., Chiasserini, D., Piersma, S.R., Knol, J.C., Möbius, W., Mollenhauer, B., van der Flier, W.M., Jimenez, C.R., Teunissen, C.E., Jahn, O., Schneider, A., 2023. C1q is increased in cerebrospinal fluid-derived extracellular vesicles in Alzheimer's disease: a multi-cohort proteomics and immuno-assay validation study. Alzheimers Dement. 19, 4828–4840. https://doi.org/10.1002/ALZ.13066.

Cizas, P., Budvytyte, R., Morkuniene, R., Moldovan, R., Broccio, M., Lösche, M., Niaura, G., Valincius, G., Borutaite, V., 2010. Size-dependent neurotoxicity of β-amyloid oligomers. Arch. Biochem. Biophys. 496, 84–92. https://doi.org/10.1016/j.abb.2010.02.001.

Cristóvaõ, J.S., Gomes, C.M., 2019. S100 proteins in Alzheimer's disease. Front. Neurosci. 13, 463. https://doi.org/10.3389/fnins.2019.00463.

Croisier, E., Moran, L.B., Dexter, D.T., Pearce, R.K.B., Graeber, M.B., 2005. Microglial inflammation in the parkinsonian substantia nigra: relationship to alpha-synuclein deposition. J. Neuroinflammation 3, 2–14. https://doi.org/10.1186/1742-2094-2-14.

Dong-Chen, X., Yong, C., Yang, X., Chen-Yu, S.T., Li-Hua, P., 2023. Signaling pathways in Parkinson's disease: molecular mechanisms and therapeutic interventions. Signal Transduct. Target. Ther. 8, 73. https://doi.org/10.1038/s41392-023-01353-3.

Dundee, J.M., Puigdellívol, M., Butler, R., Cockram, T.O.J., Brown, G.C., 2023. P2Y6 receptor-dependent microglial phagocytosis of synapses mediates synaptic and memory loss in aging. Aging Cell 22, e13761. https://doi.org/10.1111/ACEL.13761.

Dzyubenko, E., Rozenberg, A., Hermann, D.M., Faissner, A., 2016. Colocalization of synapse marker proteins evaluated by STED-microscopy reveals patterns of neuronal synapse distribution in vitro. J. Neurosci. Methods 273, 149–159. https://doi.org/10.1016/J.JNEUMETH.2016.09.001.

Fricker, M., Tolkovsky, A.M., Borutaite, V., Coleman, M., Brown, G.C., 2018. Neuronal cell death. Physiol. Rev. 98, 813–880. https://doi.org/10.1152/PHYSREV.00011.2017.

Gao, C., Jiang, J., Tan, Y., Chen, S., 2023. Microglia in neurodegenerative diseases: mechanism and potential therapeutic targets. Signal Transduct. Target. Ther. 8, 359. https://doi.org/10.1038/s41392-023-01588-0.

Garcia, V., Perera, Y.R., Chazin, W.J., 2022. A structural perspective on calprotectin as a ligand of receptors mediating inflammation and potential drug target. Biomol 12, 519. https://doi.org/10.3390/BIOM12040519.

García-Revilla, J., Boza-Serrano, A., Espinosa-Oliva, A.M., Soto, M.S., Deierborg, T., Ruiz, R., de Pablos, R.M., Burguillos, M.A., Venero, J.L., 2022. Galectin-3, a rising star in modulating microglia activation under conditions of neurodegeneration. Cell Death Dis. 13, 628. https://doi.org/10.1038/s41419-022-05058-3.

Gruden, M.A., Davydova, T.V., Wang, C., Narkevich, V.B., Fomina, V.G., Kudrin, V.S., Morozova-Roche, L.A., Sewell, R.D.E., 2016. The misfolded pro-inflammatory protein S100A9 disrupts memory via neurochemical remodelling instigating an Alzheimer's disease-like cognitive deficit. Behav. Brain Res. 306, 106–116. https://doi.org/10.1016/J.BBR.2016.03.016.

Guo, T., Zhang, D., Zeng, Y., Huang, T.Y., Xu, H., Zhao, Y., 2020. Molecular and cellular mechanisms underlying the pathogenesis of Alzheimer's disease. Mol. Neurodegener. 15, 40. https://doi.org/10.1186/S13024-020-00391-7.

Hakim-Mishnaevski, K., Flint-Brodsly, N., Shklyar, B., Levy-Adam, F., Kurant, E., 2019. Glial phagocytic receptors promote neuronal loss in adult drosophila brain. Cell Rep. 29, 1438–1448 e3. https://doi.org/10.1016/j.celrep.2019.09.086.

Hopperton, K.E., Mohammad, D., Trépanier, M.O., Giuliano, V., Bazinet, R.P., 2017. Markers of microglia in post-mortem brain samples from patients with Alzheimer's disease: a systematic review. Mol. Psychiatry 23, 177–198. https://doi.org/10.1038/mp.2017.246.

Horvath, I., Jia, X., Johansson, P., Wang, C., Moskalenko, R., Steinau, A., Forsgren, L., Wågberg, T., Svensson, J., Zetterberg, H., Morozova-Roche, L.A., 2016. Pro-inflammatory S100A9 protein as a robust biomarker differentiating early stages of cognitive impairment in Alzheimer's disease. ACS Chem. Neurosci. 7, 34–39. https://doi.org/10.1021/acschemneuro.5b00265.

Horvath, I., Iashchishyn, I.A., Moskalenko, R.A., Wang, C., Wärmländer, S.K.T.S., Wallin, C., Gräslund, A., Kovacs, G.G., Morozova-Roche, L.A., 2018. Co-aggregation of pro-inflammatory S100A9 with α-synuclein in Parkinson's disease: ex vivo and in vitro studies. J. Neuroinflammation 15, 172. https://doi.org/10.1186/s12974-018-1210-9.

Hunter, M.J., Chazin, W.J., 1998. High level expression and dimer characterization of the S100 EF-hand proteins, migration inhibitory factor-related proteins 8 and 14. J. Biol. Chem. 273, 12427–12435. https://doi.org/10.1074/JBC.273.20.12427.

Jebelli, J., Piers, T., Pocock, J., 2015. Selective depletion of microglia from cerebellar granule cell cultures using L-leucine methyl ester. J. Vis. Exp. 101, e52983. https://doi.org/10.3791/52983.

Kim, H.J., Chang, K.A., Ha, T.Y., Kim, J., Ha, S., Shin, K.Y., Moon, C., Nacken, W., Kim, H.S., Suh, Y.H., 2014. S100A9 knockout decreases the memory impairment and neuropathology in crossbreed mice of Tg2576 and S100A9 knockout mice model. PLoS One 9, e88924. https://doi.org/10.1371/JOURNAL.PONE.0088924.

Kinsner, A., Boveri, M., Hareng, L., Brown, G.C., Coecke, S., Hartung, T., Bal-Price, A., 2006. Highly purified lipoteichoic acid induced pro-inflammatory signalling in primary culture of rat microglia through toll-like receptor 2: selective potentiation of nitric oxide production by muramyl dipeptide. J. Neurochem. 99, 596–607. https://doi.org/10.1111/j.1471-4159.2006.04085.x.

Kouli, A., Camacho, M., Allinson, K., Williams-Gray, C.H., 2020. Neuroinflammation and protein pathology in Parkinson's disease dementia. Acta Neuropathol. Commun. 8, 211. https://doi.org/10.1186/S40478-020-01083-5.

Kummer, M.P., Vogl, T., Axt, D., Griep, A., Vieira-Saecker, A., Jessen, F., Gelpi, E., Roth, J., Heneka, M.T., 2012. Mrp14 deficiency ameliorates amyloid β burden by increasing microglial phagocytosis and modulation of amyloid precursor protein processing. J. Neurosci. 32, 17824–17829. https://doi.org/10.1523/JNEUROSCI.1504-12.2012.

Kwon, S., Iba, M., Kim, C., Masliah, E., 2020. Immunotherapies for aging-related neurodegenerative diseases—emerging perspectives and new targets. Neurotherapeutics 17, 935–954. https://doi.org/10.1007/S13311-020-00853-2.

Liu, P., Wang, Y., Sun, Y., Peng, G., 2022. Neuroinflammation as a potential therapeutic target in Alzheimer's disease. Clin. Interv. Aging 17, 665–674. https://doi.org/10.2147/CIA.S357558.

Milde, S., Brown, G.C., 2022. Knockout of the P2Y6 receptor prevents peri-infarct neuronal loss after transient, focal ischemia in mouse brain. Int. J. Mol. Sci. 23, 2304. https://doi.org/10.3390/IJMS23042304.

Milde, S., van Tartwijk, F.W., Vilalta, A., Hornik, T.C., Dundee, J.M., Puigdellívol, M., Brown, G.C., 2021. Inflammatory neuronal loss in the substantia nigra induced by systemic lipopolysaccharide is prevented by knockout of the P2Y6 receptor in mice. J. Neuroinflammation 18, 225. https://doi.org/10.1186/s12974-021-02280-2.

Minett, T., Classey, J., Matthews, F.E., Fahrenhold, M., Taga, M., Brayne, C., Ince, P.G., Nicoll, J.A.R., Boche, D., 2016. Microglial immunophenotype in dementia with Alzheimer's pathology. J. Neuroinflammation 13, 135. https://doi.org/10.1186/s12974-016-0601-z.

Neher, J.J., Neniskyte, U., Zhao, J.-W., Bal-Price, A., Tolkovsky, A.M., Brown, G.C., 2011. Inhibition of microglial phagocytosis is sufficient to prevent inflammatory neuronal death. J. Immunol. 186, 4973–4983. https://doi.org/10.4049/jimmunol.1003600.

Neher, J.J., Emmrich, J.V., Fricker, M., Mander, P.K., Thery, C., Brown, G.C., 2013. Phagocytosis executes delayed neuronal death after focal brain ischemia. Proc. Natl. Acad. Sci. 110, E4098–E40107. https://doi.org/10.1073/pnas.1308679110.

Neniskyte, U., Brown, G.C., 2013a. Lactadherin/MFG-E8 is essential for microglia-mediated neuronal loss and phagoptosis induced by amyloid β. J. Neurochem. 126, 312–317. https://doi.org/10.1111/jnc.12288.

Neniskyte, U., Brown, G.C., 2013b. Analysis of microglial production of reactive oxygen and nitrogen species. Methods Mol. Biol. 1041, 103–111. https://doi.org/10.1007/978-1-62703-520-0_12.

Neniskyte, U., Neher, J.J., Brown, G.C., 2011. Neuronal death induced by nanomolar amyloid β is mediated by primary phagocytosis of neurons by microglia. J. Biol. Chem. 286, 39904–39913. https://doi.org/10.1074/jbc.M111.267583.

Neniskyte, U., Vilalta, A., Brown, G.C., 2014. Tumour necrosis factor alpha-induced neuronal loss is mediated by microglial phagocytosis. FEBS Lett. 588, 2952–2956. https://doi.org/10.1016/j.febslet.2014.05.046.

Neniskyte, U., Fricker, M., Brown, G.C., 2016. Amyloid β induces microglia to phagocytose neurons via activation of protein kinase Cs and NADPH oxidase. Int. J. Biochem. Cell Biol. 81, 346–355. https://doi.org/10.1016/j.biocel.2016.06.005.

Pampuscenko, K., Morkuniene, R., Sneideris, T., Smirnovas, V., Budvytyte, R., Valincius, G., Brown, G.C., Borutaite, V., 2020. Extracellular tau induces microglial phagocytosis of living neurons in cell cultures. J. Neurochem. 154, 316–329. https://doi.org/10.1111/jnc.14940.

Pampuscenko, K., Morkuniene, R., Krasauskas, L., Smirnovas, V., Tomita, T., Borutaite, V., 2021. Distinct neurotoxic effects of extracellular tau species in primary neuronal-glial cultures. Mol. Neurobiol. 58, 658–667. https://doi.org/10.1007/s12035-020-02150-7.

Pampuscenko, K., Morkuniene, R., Krasauskas, L., Smirnovas, V., Brown, G.C., Borutaite, V., 2023. Extracellular tau stimulates phagocytosis of living neurons by activated microglia via toll-like 4 receptor-NLRP3 inflammasome-caspase-1 signalling axis. Sci. Rep. 13, 10813. https://doi.org/10.1038/S41598-023-37887-3.

Podleśny-Drabiniok, A., Marcora, E., Goate, A.M., 2020. Microglial phagocytosis: a disease-associated process emerging from Alzheimer's disease genetics. Trends Neurosci. 43, 965–979. https://doi.org/10.1016/J.TINS.2020.10.002.

Puigdellívol, M., Milde, S., Vilalta, A., Cockram, T.O.J., Allendorf, D.H., Lee, J.Y., Dundee, J.M., Pampuščenko, K., Borutaite, V., Nuthall, H.N., Brelstaff, J.H., Spillantini, M.G., Brown, G.C., 2021. The microglial P2Y 6 receptor mediates neuronal loss and memory deficits in neurodegeneration. Cell Rep. 37, 110148. https://doi.org/10.1016/J.CELREP.2021.110148.

Rueda-Carrasco, J., Sokolova, D., Lee, S., Childs, T., Jurčáková, N., Crowley, G., De Schepper, S., Ge, J.Z., Lachica, J.I., Toomey, C.E., Freeman, O.J., Hardy, J., Barnes, S.J., Lashley, T., Stevens, B., Chang, S., Hong, S., 2023. Microglia-synapse engulfment via PtdSer-TREM2 ameliorates neuronal hyperactivity in Alzheimer's disease models. EMBO J. 42, e113246. https://doi.org/10.15252/embj.2022113246.

Russo, A., Schürmann, H., Brandt, M., Scholz, K., Matos, A.L.L., Grill, D., Revenstorff, J., Rembrink, M., von Wulffen, M., Fischer-Riepe, L., Hanley, P.J., Häcker, H., Prünster, M., Sánchez-Madrid, F., Hermann, S., Klotz, L., Gerke, V., Betz, T., Vogl, T., Roth, J., 2022. Alarming and calming: opposing roles of S100A8/S100A9 dimers and tetramers on monocytes. Adv. Sci. 9, e2201505. https://doi.org/10.1002/ADVS.202201505.

Schneider, C.A., Rasband, W.S., Eliceiri, K.W., 2012. NIH Image to ImageJ: 25 years of image analysis. Nat. Methods 9, 671–675. https://doi.org/10.1038/nmeth.2089.

Scott-Hewitt, N., Perrucci, F., Morini, R., Erreni, M., Mahoney, M., Witkowska, A., Carey, A., Faggiani, E., Schuetz, L.T., Mason, S., Tamborini, M., Bizzotto, M., Passoni, L., Filipello, F., Jahn, R., Stevens, B., Matteoli, M., 2020. Local externalization of phosphatidylserine mediates developmental synaptic pruning by microglia. EMBO J. 39, e105380. https://doi.org/10.15252/EMBJ.2020105380.

Shepherd, C.E., Goyette, J., Utter, V., Rahimi, F., Yang, Z., Geczy, C.L., Halliday, G.M., 2006. Inflammatory S100A9 and S100A12 proteins in Alzheimer's disease. Neurobiol. Aging 27, 1554–1563. https://doi.org/10.1016/J.NEUROBIOLAGING.2005.09.033.

Shimizu, T., Schutt, C.R., Izumi, Y., Tomiyasu, N., Omahdi, Z., Kano, K., Takamatsu, H., Aoki, J., Bamba, T., Kumanogoh, A., Takao, M., Yamasaki, S., 2023. Direct activation of microglia by β-glucosylceramide causes phagocytosis of neurons that exacerbates Gaucher disease. Immunity 56, 307–319 e8. https://doi.org/10.1016/J.IMMUNI.2023.01.008.

Shin, H.W., Takatsu, H., 2020. Phosphatidylserine exposure in living cells. Crit. Rev. Biochem. Mol. Biol. 55, 166–178. https://doi.org/10.1080/10409238.2020.1758624.

Shlomovitz, I., Speir, M., Gerlic, M., 2019. Flipping the dogma - phosphatidylserine in non-apoptotic cell death. Cell Commun. Signal. 7, 139. https://doi.org/10.1186/s12964-019-0437-0.

Sinha, A., Kushwaha, R., Molesworth, K., Mychko, O., Makarava, N., Baskakov, I.V., 2021. Phagocytic activities of reactive microglia and astrocytes associated with prion diseases are dysregulated in opposite directions. Cells 10, 1728. https://doi.org/10.3390/CELLS10071728.

Studier, F.W., 2005. Protein production by auto-induction in high density shaking cultures. Protein Expr. Purif. 41, 207–234. https://doi.org/10.1016/J.PEP.2005.01.016.

Suzuki, J., Umeda, M., Sims, P.J., Nagata, S., 2010. Calcium-dependent phospholipid scrambling by TMEM16F. Nature 468, 834–840. https://doi.org/10.1038/NATURE09583.

Swindell, W.R., Johnston, A., Xing, X., Little, A., Robichaud, P., Voorhees, J.J., Fisher, G., Gudjonsson, J.E., 2013. Robust shifts in S100a9 expression with aging: a novel mechanism for chronic inflammation. Sci. Rep. 3, 1215. https://doi.org/10.1038/SREP01215.

Tremblay, M.E., Cookson, M.R., Civiero, L., 2019. Glial phagocytic clearance in Parkinson's disease. Mol. Neurodegener. 14, 16. https://doi.org/10.1186/S13024-019-0314-8.

Umpierre, A.D., Li, B., Ayasoufi, K., Simon, W.L., Zhao, S., Xie, M., Thyen, G., Hur, B., Zheng, J., Liang, Y., Bosco, D.B., Maynes, M.A., Wu, Z., Yu, X., Sung, J., Johnson, A. J., Li, Y., Wu, L.J., 2024. Microglial P2Y6 calcium signaling promotes phagocytosis and shapes neuroimmune responses in epileptogenesis. Neuron 112, 1959–1977 e10. https://doi.org/10.1016/j.neuron.2024.03.017.

Wang, C., Klechikov, A.G., Gharibyan, A.L., Wärmländer, S.K.T.S., Jarvet, J., Zhao, L., Jia, X., Shankar, S.K., Olofsson, A., Brännström, T., Mu, Y., Gräslund, A., Morozova-Roche, L.A., 2014. The role of pro-inflammatory S100A9 in Alzheimer's disease amyloid-neuroinflammatory cascade. Acta Neuropathol. 127, 507–522. https://doi.org/10.1007/S00401-013-1208-4.

Wang, C., Iashchishyn, I.A., Pansieri, J., Nyström, S., Klementieva, O., Kara, J., Horvath, I., Moskalenko, R., Rofougaran, R., Gouras, G., Kovacs, G.G., Shankar, S.K., Morozova-Roche, L.A., 2018a. S100A9-driven amyloid-neuroinflammatory cascade in traumatic brain injury as a precursor state for Alzheimer's disease. Sci. Report. 8, 12836. https://doi.org/10.1038/s41598-018-31141-x.

Wang, S., Song, R., Wang, Z., Jing, Z., Wang, Shaoxiong, Ma, J., 2018b. S100A8/A9 in inflammation. Front. Immunol. 9, 371351. https://doi.org/10.3389/fimmu.2018.01298.

Wang, G., Huang, K., Tian, Q., Guo, Y., Liu, C., Li, Z., Yu, Z., Zhang, Z., Li, M., 2024. S100A9 aggravates early brain injury after subarachnoid hemorrhage via inducing neuroinflammation and inflammasome activation. iScience 27, 109165. https://doi.org/10.1016/J.ISCI.2024.109165.

Wilson, D.M., Cookson, M.R., Van Den Bosch, L., Zetterberg, H., Holtzman, D.M., Dewachter, I., 2023. Hallmarks of neurodegenerative diseases. Cell 186, 693–714. https://doi.org/10.1016/J.CELL.2022.12.032.

Wu, T., Dejanovic, B., Gandham, V.D., Gogineni, A., Edmonds, R., Schauer, S., Srinivasan, K., Huntley, M.A., Wang, Y., Wang, T.M., Hedehus, M., Barck, K.H., Stark, M., Ngu, H., Foreman, O., Meilandt, W.J., Elstrott, J., Chang, M.C., Hansen, D. V., Carano, R.A.D., Sheng, M., Hanson, J.E., 2019. Complement C3 is activated in human AD brain and is required for neurodegeneration in mouse models of amyloidosis and tauopathy. Cell Rep. 28, 2111–2123.e6. https://doi.org/10.1016/J.CELREP.2019.07.060.

Xiao, B., Tan, E.K., 2023. Immunotherapy trials in Parkinson's disease: challenges. J. Transl. Med. 21, 178. https://doi.org/10.1186/s12967-023-04012-x.

Zhang, X., Sun, D., Zhou, X., Zhang, C., Yin, Q., Chen, L., Tang, Y., Liu, Y., Morozova-Roche, L.A., 2023a. Proinflammatory S100A9 stimulates TLR4/NF-κB signaling pathways causing enhanced phagocytic capacity of microglial cells. Immunol. Lett. 255, 54–61. https://doi.org/10.1016/J.IMLET.2023.02.008.

Zhang, W., Xiao, D., Mao, Q., Xia, H., 2023b. Role of neuroinflammation in neurodegeneration development. Signal Transduct. Target. Ther. 8, 267. https://doi.org/10.1038/S41392-023-01486-5.

Zhao, L., Zabel, M.K., Wang, X., Ma, W., Shah, P., Fariss, R.N., Qian, H., Parkhurst, C.N., Gan, W., Wong, W.T., 2015. Microglial phagocytosis of living photoreceptors contributes to inherited retinal degeneration. EMBO Mol. Med. 7, 1179–1197. https://doi.org/10.15252/emmm.201505298.

Ziegler, G., Prinz, V., Albrecht, M.W., Harhausen, D., Khojasteh, U., Nacken, W., Endres, M., Dirnagl, U., Nietfeld, W., Trendelenburg, G., 2009. Mrp-8 and -14 mediate CNS injury in focal cerebral ischemia. Biochim. Biophys. Acta Mol. basis Dis. 1792, 1198–1204. https://doi.org/10.1016/J.BBADIS.2009.10.003.